Variational-average-atom-in-quantum-plasmas (VAAQP) code and virial theorem: Equation-of-state and shock-Hugoniot calculations for warm dense Al, Fe, Cu, and Pb

R. Piron[1,*] and T. Blenski[2]
[1]*CEA, DAM, DIF, F-91297 Arpajon, France*
[2]*CEA, IRAMIS, Service des Photons Atomes et Molécules, F-91191 Gif-sur-Yvette, France*
(Received 13 October 2010; published 9 February 2011)

The numerical code VAAQP (variational average atom in quantum plasmas), which is based on a fully variational model of equilibrium dense plasmas, is applied to equation-of-state calculations for aluminum, iron, copper, and lead in the warm-dense-matter regime. VAAQP does not impose the neutrality of the Wigner-Seitz ion sphere; it provides the average-atom structure and the mean ionization self-consistently from the solution of the variational equations. The formula used for the electronic pressure is simple and does not require any numerical differentiation. In this paper, the virial theorem is derived in both nonrelativistic and relativistic versions of the model. This theorem allows one to express the electron pressure as a combination of the electron kinetic and interaction energies. It is shown that the model fulfills automatically the virial theorem in the case of local-density approximations to the exchange-correlation free-energy. Applications of the model to the equation-of-state and Hugoniot shock adiabat of aluminum, iron, copper, and lead in the warm-dense-matter regime are presented. Comparisons with other approaches, including the INFERNO model, and with available experimental data are given. This work allows one to understand the thermodynamic consistency issues in the existing average-atom models. Starting from the case of aluminum, a comparative study of the thermodynamic consistency of the models is proposed. A preliminary study of the validity domain of the INFERNO model is also included.

DOI: 10.1103/PhysRevE.83.026403 PACS number(s): 52.25.Kn, 52.25.Jm, 52.27.Gr

I. INTRODUCTION

Theoretical models of matter at high-energy-density, typically $10^{11}\,\mathrm{J\,m^{-3}}$ and beyond, became necessary in the 1930s in the context of astrophysics. The problem of opacity was addressed, for example, by Rosseland in 1930 [1]. Since then, interest in this problem has remained constant, and ever more elaborate approaches have appeared (see, for example, [2–4]). Like opacity, the equation-of-state (EOS) was the object of constant efforts (see, for example, Refs. [5,6]).

While the need for models of matter at high-energy-density is still of great interest in astrophysics, other fields of applications have appeared. Among these are inertial confinement fusion (ICF, see Refs. [7,8]), the realization of x-ray sources (see Refs. [9,10]), and the interpretation of xuv spectroscopy experiments (see Refs. [11,12]).

These various applications usually involve matter densities from a fraction of solid density to several hundred times solid density, at temperatures between a few electron volts to tens of kiloelectron volts.

In this paper, we address plasmas in local thermodynamic equilibrium (LTE) where the ions are moderately or strongly coupled ($\Gamma > 1$, $\Gamma \gg 1$), and electrons are partially or totally degenerate ($k_B T \lesssim E_F$). Free electrons are taken to be nonrelativistic in the sense that ($k_B T \ll mc^2$). However, elements taken into account can be heavy and may require a relativistic wave equation for atomic electrons. These plasmas are typical for ICF and astrophysics and combine aspects of hot matter, such as ionization and fluid behavior, and aspects of cold matter, such as electron degeneracy.

In the theoretical context that we have just expressed, we can consider treating bound electrons with various degrees of complexity and precision. We can account for the detailed atomic levels that exist in the plasma, consider configuration averages, superconfiguration averages [13], or even only consider the mean configuration of an atom. In this last case, we deal with what is called an average atom. All these methods rely on a common theoretical basis that is a particular concept of an atom in a plasma. This concept is not obvious and several difficulties are inherently connected to its formulation.

Among the first approaches to atoms in plasmas, the most important and still very useful is the Thomas-Fermi (TF) model at finite temperature proposed by Feynman, Metropolis, and Teller in Ref. [14]. In this model, the atom may be viewed as confined to the Wigner-Seitz (WS) sphere, which is immersed in a homogeneous jellium composed of delocalized electrons neutralized by a uniform ion background. At low temperatures, however, the TF WS atomic sphere may also be considered as an approximation to the basic cell of a periodic solid (see, for instance, Ref. [15]). In the TF model, calculations are performed inside the WS sphere, resulting in the self-consistent-field potential and electron density. They provide also the homogeneous electron or jellium density beyond the WS radius, obtained as the boundary value of the TF electron density at the WS radius. The jellium density provides the chemical potential and the average number of delocalized electrons per atom. The TF model has an important feature which is the thermodynamic consistency. That means it can be obtained from a variational minimization of the system free-energy and fulfills the virial theorem. This theorem allows one to express the electron pressure as a combination of the electron kinetic and interaction energies. Thus in the case of the TF model, the variational approach provides the plasma electronic structure and the average ionization simultaneously.

*robin.piron@cea.fr

However, being quasiclassical, the model does not lead to any shell structure. Nevertheless, potentials obtained from this model have sometimes been used to calculate wave functions connected to radiative properties of plasmas (see Refs. [3,16]). Some works have also been performed to include shell effects in the TF model (see, for example, Refs. [17–19]).

A first comprehensive and useful self-consistent quantum extension of the TF model was the average-atom model of Rozsnyai (see Ref. [20]). In this model, the bound electrons are treated quantum mechanically while the delocalized electron population is still treated as a TF fluid. Such a dual approach to electrons makes a variational derivation of Rozsnyai's model impossible, leads to discontinuities in thermodynamic quantities, and is one of the reasons for the violation of the virial theorem in this model. Due to its relative simplicity, Rozsnyai's model has been used in many approximate approaches to plasma radiative properties or as a starting point in detailed configuration codes.

The first purely quantum approach to an average atom in plasma is Liberman's INFERNO model (see Ref. [21]). In Liberman's model, the WS sphere appears explicitly as the cavity into which noncentral ions do not enter. The delocalized electrons are treated quantum mechanically in the INFERNO model, which would result, in principle, in Friedel-type oscillations of the self-consistent electron density and potential extending beyond the WS radius. However, in the model, these oscillations are disregarded beyond the WS sphere, with the potential and density consequently approximated as homogeneous. This assumption implies the neutrality of the WS sphere. Both the confined-atom aspect and the WS sphere neutrality introduced in this model (in analogy to the TF model) imply that from a formal point of view, the INFERNO model does not have a variational character (see Refs. [22–25]). It appears that this nonvariational character of the model may have some practical implications, although probably only in a rather restrained region of plasma temperatures and densities (see Sec. IV). Recently, a new version of the INFERNO model, called PURGATORIO, was developed by Wilson and his collaborators (see Refs. [26,27]).

Perrot proposed [28] an improved quantum average atom in plasma model by eliminating the requirement of the WS sphere neutrality. In his AJCI ("Atome dans le Jellium de Charge Imposée," that is, atom-in-jellium with imposed charge) model, the self-consistent potential and electron density are considered in the whole space with the condition that the potential is screened. This corresponds to the neutrality condition in the whole space. The concept of the WS cavity where the noncentral ions are absent is preserved in the AJCI model. However, the formulation of the AJCI model does not provide the ion mean charge or, in other words, the jellium density of the surrounding medium. For that reason, one has to impose in the model the mean ion charge, which explains the origin of its name. In practice, it was usually set to the value stemming from the TF model. This fact suggested that something was missing in the AJCI model. This problem was solved in Refs. [22,23], in which the presence of the zero-order free-energy term in the cluster expansion provided the lacking variational equation for the average mean charge. The first practical realization of the new variational model of Refs. [22,23] was reported in Refs. [24,25]. In these two last publications, the ionization model, which was introduced in Refs. [22,23] as a postulate, was found to have the meaning of the cluster expansion of the total number of electrons per atom. This observation simplified the model and made it more consistent. In the new formulation, the model simply relies on the cluster expansions of two observable quantities: the average free-energy per ion and the total number of electrons per ion.

In this paper, we apply the VAAQP code, which is based on the ideas developed in Refs. [22–25], to equation-of-state calculations. The theory is outlined in Sec. II. The numerical method and main options of the code are presented in Sec. III. The EOS results, mainly in form of the mean ionization in the case of aluminum, iron, copper, and lead in the warm-dense-matter (WDM) regime, are displayed in Sec. IV. This section also contains comparisons with results from the INFERNO and the Thomas-Fermi-Dirac (TFD) models. Hugoniot shock adiabats for the same materials are presented in Sec. V, together with comparisons to results from the INFERNO and TFD versions of the code as well as with available experimental data. Section VI contains the direct proof of the virial theorem in both relativistic and nonrelativistic cases. Following Ref. [14], a sketch of a proof of the virial theorem based on the scaling properties was proposed for the nonrelativistic case in Ref. [22]. During work on the code, it became necessary to calculate and control directly all virial contributions as well as to check the virial theorem. It became important also to verify if the virial theorem is fulfilled whatever the choice of the local-density exchange correlation free-energy. We show in Sec. VI that the virial and thermodynamic pressures are identical if the variational equations of the model are respected. An important result is the fact that the proof remains true for all forms of the local-density exchange-correlation term, and that this statement holds in both the relativistic and nonrelativistic cases. The problem of the exchange-correlation contribution to pressure in the case of high-temperature compressed matter remains an important issue (see, for instance, [29]). Recently, there have been some continuous efforts aimed at developing a new EOS model for the Super-Transition Arrays (STA) code (the so-called EOSTA approach; see Refs. [30–32]). The starting point in this new EOS is the INFERNO-type model. In this approach, a new exchange-correlation potential is constructed from the requirement that the thermodynamic and virial pressures be equal. We think that our proof and considerations from Sec. VI may allow one to better understand the EOSTA approach and its limitations. Section VII contains conclusions.

II. OUTLINE OF THE VARIATIONAL-AVERAGE-ATOM-IN-QUANTUM-PLASMAS (VAAQP) MODEL

A. Cluster expansion

We consider a plasma composed of ions of element having atomic number Z at local thermodynamic equilibrium (LTE) characterized by the temperature T and the ion density n_i. Let us consider the electron free-energy per unit volume averaged over all possible ion distributions. We may perform a cluster expansion of this free-energy density and retain only the first

two terms of this expansion (see Refs. [22–25] and references therein for more details):

$$f = f_0 + \langle f \rangle_1 + \cdots . \tag{1}$$

The zeroth-order term f_0 corresponds to the free-energy per unit volume of a uniform electron gas with a density n_0 that is unknown and has to be determined from the model. The first-order term $\langle f \rangle_1$ corresponds to the averaged contributions of all one-center ions and has the form

$$\langle f \rangle_1 = n_i \int d^3r \big\{ f_1^{\rm jel}\{n_0, X; n_i, Z, T, e^2, m; \boldsymbol{r}\} - f_0(n_0; n_i, Z, T, e^2, m) \big\} = n_i \Delta F_1, \tag{2}$$

where $f_1^{\rm jel}$ is the free-energy per unit volume of the system composed of a central ion immersed in an infinite jellium. By X we denote all internal structure variables of the ion. In the preceding expression, according to the cluster-expansion technique, the zeroth-order term is subtracted, which assures the convergence of the integral. It is worth noting that we display explicitly the dependence of functionals on the squared electron charge e^2 as well as on the electron mass m. These dependences will be needed in Sec. VI.

We limit ourselves to the treatment of the cluster expansion up to the first-order term, which means that we only consider effects of up to one central ion. This hypothesis may be viewed as defining the framework of the atomic physics of plasmas.

In the present paper, we study the electrons in the framework of the density-functional theory (DFT), as defined in Ref. [33]. For that reason, we can assume that all internal structure variables previously denoted by X reduce to the electron density $n(\boldsymbol{r})$ or equivalently to the trial potential $v(\boldsymbol{r})$ corresponding to that density. For the sake of simplicity, our choice is to construct the free-energy functional using $v(\boldsymbol{r})$ as the unknown variable. Consequently, the notation $n(\boldsymbol{r})$ that we will use for the electron density is to be understood as a shorthand notation for the functional $n\{n_0, v(\boldsymbol{r}'); T, m; \boldsymbol{r}\}$. Once the full dependence of a functional has been stated, we will often omit it in order to shorten the notation.

From Eq. (1), we can write the free energies per ion as follows:

$$F\{n_0, v(\boldsymbol{r}); n_i, Z, T, e^2, m\} \equiv F_0(n_0; n_i, T, e^2, m) + \Delta F_1\{n_0, v(\boldsymbol{r}); n_i, Z, T, e^2, m\}, \tag{3}$$

where $F_0 = f_0(n_0; T, e^2, m)/n_i$. We treat the ΔF_1 contribution according to the so-called Mermin-Kohn-Sham formalism (see Refs. [34,35]),

$$\Delta F_1 \equiv \Delta F_1^0\{n_0, v(\boldsymbol{r}); T, m\} + \Delta F_1^{\rm el}\{n_0, v(\boldsymbol{r}); n_i, Z, T, e^2, m\} + \Delta F_1^{\rm xc}\{n_0, v(\boldsymbol{r}); T, e^2, m\}. \tag{4}$$

ΔF_1^0 is the kinetic-entropic contribution to the free-energy of a system of noninteracting electrons, $\Delta F_1^{\rm el}$ is the electrostatic part of the free-energy, and $\Delta F_1^{\rm xc}$ is the exchange-correlation part.

We may also perform the cluster expansion of the total number of electrons per ion taking into account only the first two terms of this expansion (see again [22–25] and references therein):

$$Z = Z^* + \langle Z \rangle_1 + \cdots . \tag{5}$$

The zeroth-order term $Z^* = n_0/n_i$ corresponds to the average number of free electrons per ion, which has to be determined from the model. The first-order term $\langle Z \rangle_1$ corresponds to the averaged contributions to bound electrons per ion coming from all one-center ions and has the form

$$\langle Z \rangle_1 = n_i \int d^3r \{ n\{n_0, X; n_i, Z, T, e^2, m; \boldsymbol{r}\} - n_0 \}. \tag{6}$$

B. DFT expression of the free-energy

We denote by $\tilde{H}$ the general one-body Hamiltonian operator. In the nonrelativistic case, $\tilde{H}$ is the Schrödinger Hamiltonian operator $\tilde{H}_S$,

$$\tilde{H}_S \equiv \frac{\tilde{P}^2}{2m} - \tilde{V}, \tag{7}$$

where $\tilde{\mathbf{P}}$ is the momentum operator and $\tilde{V}$ is the trial potential operator such as, in the Dirac notation, $\tilde{V}|\boldsymbol{r}\rangle = |\boldsymbol{r}\rangle v(\boldsymbol{r})$. In the relativistic case, $\tilde{H}$ is the Dirac Hamiltonian operator $\tilde{H}_D$,

$$\tilde{H}_D \equiv \tilde{T} + (\beta - \mathbb{I})mc^2 - \tilde{V}\ ;\ \tilde{T} \equiv \boldsymbol{\alpha} \cdot \tilde{\boldsymbol{P}} c, \tag{8}$$

where $\boldsymbol{\alpha}$,β are the Dirac matrices. The relativistic extension of the DFT formalism is addressed in Refs. [36,37]. We also define the generic notation for the Hamiltonian operators of the free electrons,

$$\tilde{H}^0 \equiv \tilde{H} + \tilde{V}. \tag{9}$$

We denote by $\{\{|\varphi_j\rangle\}, \{|\varphi_{\mathbf{k},s}\rangle\}\}$ the basis constituted by the eigenstates of $\tilde{H}$. This basis is composed of the discrete $\{|\varphi_j\rangle\}$ and continuum $\{|\varphi_{\mathbf{k},s}\rangle\}$ eigenstates. In the nonrelativistic case, the $|r\rangle$ representations $\varphi_{\mathbf{k},s}(\boldsymbol{r})$ of these eigenstates are wave functions independent of the spin indices s, which can be omitted. In the relativistic case, we disregard the negative energy states (as in Refs. [36,37]), and the $|r\rangle$ representations $\varphi_{\mathbf{k},s}(\boldsymbol{r})$ of the eigenstates are Dirac bispinors. To denote the Hermitian conjugate of $\varphi_{\mathbf{k},s}(\boldsymbol{r})$, we use the generic notation $\varphi^c_{\mathbf{k},s}(\boldsymbol{r})$. In the nonrelativistic case $\varphi^c_{\mathbf{k},s}(\boldsymbol{r}) = \varphi^*_{\mathbf{k}}(\boldsymbol{r})$, whereas in the relativistic case $\varphi^c_{\mathbf{k},s}(\boldsymbol{r}) = \varphi^\dagger_{\mathbf{k},s}(\boldsymbol{r})$. We denote by $\{|\varphi^0_{\mathbf{k},s}\rangle\}$ the basis constituted by the eigenstates of $\tilde{H}^0$.

The kinetic-entropic contribution to the free-energy can be expressed as follows:

$$\Delta F_1^0 = g_s \sum_j \int d^3r \big\{ f^F_{n_0,T}(E_j)\varphi^c_j(\boldsymbol{r}) H^0 \varphi_j(\boldsymbol{r}) - T S_{n_0,T}(E_j)|\varphi_j(\boldsymbol{r})|^2 \big\} + g_s \sum\!\!\!\!\!\!\int \frac{d^3k}{(2\pi)^3} \int d^3r \big\{ f^F_{n_0,T}(E_k)\varphi^c_{\mathbf{k},s}(\boldsymbol{r}) H^0 \varphi_{\mathbf{k},s}(\boldsymbol{r}) - T S_{n_0,T}(E_k)|\varphi_{\mathbf{k},s}(\boldsymbol{r})|^2 - f^F_{n_0,T}(E_k)\varphi^{0\,c}_{\mathbf{k},s}(\boldsymbol{r}) H^0 \varphi^0_{\mathbf{k},s}(\boldsymbol{r}) + T S_{n_0,T}(E_k)\big|\varphi^0_{\mathbf{k},s}(\boldsymbol{r})\big|^2 \big\}, \tag{10}$$

where $f^F_{n_0,T}(E) = (e^{(E-\mu_{n_0})/(k_BT)}+1)^{-1}$ is the Fermi-Dirac distribution related to the chemical potential μ_{n_0} such that

$$\int_0^\infty dE\left\{f^F_{n_0,T}(E)\right\} = n_0 \tag{11}$$

and

$$S_{n_0,T}(E) \equiv -k_B\left(f^F_{n_0,T}(E)\ln\left(f^F_{n_0,T}(E)\right) + \left(1-f^F_{n_0,T}(E)\right)\ln\left(1-f^F_{n_0,T}(E)\right)\right). \tag{12}$$

The sum-integral symbol in Eq. (10) denotes the sum on the spin index s in the relativistic case, and g_s is the spin-degeneracy factor (1 in the relativistic case, 2 in the nonrelativistic case).

The electrostatic part of the free-energy $\Delta F_1^{\rm el}$ can be written as

$$\Delta F_1^{\rm el} = e^2\int d^3r'\left\{(n(r')-n_0G(r'))\times\left(-\frac{Z}{r'}+\frac{1}{2}\int d^3r''\left\{\frac{n(r'')-n_0G(r'')}{|\boldsymbol{r}'-\boldsymbol{r}''|}\right\}\right)\right\}, \tag{13}$$

where $n_0G(r)$ corresponds to the noncentral-ion charge density. In this way, first-order contribution to the cluster expansion then involves the second-order ion-ion correlation function $G(r)$. We approximate $G(r)$ by the Heaviside function $\theta(r-R)$, with a radius R. This constitutes a rather crude approximation of the ion-ion correlation function corresponding to a coupling parameter $\Gamma\sim 5$ (see, for example, Ref. [38]), where $\Gamma \equiv Z^{*2}/(k_BTR^{n_i}_{\rm WS})$. The noncentral ions are thus supposed to form a homogeneous charge background of a density n_0, which does not enter into a sphere of a radius R. The function $G(r)$ in such simplified form corresponds to the idea of a cavity first introduced by Liberman in the INFERNO model, which, however, has been present in practically all models of atoms in plasmas. The condition of overall charge neutrality then reads

$$Z-\int d^3r\{n(\boldsymbol{r})-n_0\theta(r-R)\} = 0. \tag{14}$$

From the comparison of the neutrality condition Eq. (14) with Eq. (5), it follows that R must be the WS radius,

$$R = R^{n_i}_{\rm WS} = \left(\frac{3}{4\pi n_i}\right)^{1/3}. \tag{15}$$

In the framework of the local-density-approximation (LDA), the exchange-correlation part of the free-energy $\Delta F_1^{\rm xc}$ can be written as

$$\Delta F_1^{\rm xc} = \int d^3r\{f_{\rm xc}(n(r),T,e^2,m)-f_{\rm xc}(n_0,T,e^2,m)\}, \tag{16}$$

where $f_{\rm xc}(n,T,e^2,m)$ is the exchange-correlation free-energy density function (see, for instance, Ref. [39]). We denote by $v_{\rm xc}(n,T,e^2,m)$ the exchange-correlation potential, namely,

$$v_{\rm xc}(n,T,e^2,m) \equiv \frac{\partial f_{\rm xc}(n,T,e^2,m)}{\partial n}. \tag{17}$$

C. Minimization of the free-energy

We minimize the functional F with respect to its dependences on n_0, $v(\boldsymbol{r})$, with the additional constraint of overall charge neutrality [Eqs. (14) and (15)].

We thus define the functional Ω as follows:

$$\Omega\{n_0,v(\boldsymbol{r});n_i,Z,T,e^2,m\} \equiv F\{n_0,v(\boldsymbol{r});n_i,Z,T,e^2,m\} - \gamma\left(Z-\int d^3r\left\{n(\boldsymbol{r})-n_0\theta\left(r-R^{n_i}_{\rm WS}\right)\right\}\right), \tag{18}$$

where γ is a Lagrange multiplier. To find the thermodynamic equilibrium, we have to fulfill the equations

$$\frac{\delta\Omega\{n_0,v(\boldsymbol{r});n_i,Z,T,e^2,m\}}{\delta v(\boldsymbol{r})} = 0, \tag{19}$$

$$\frac{\delta\Omega\{n_0,v(\boldsymbol{r});n_i,Z,T,e^2,m\}}{\delta n_0} = 0. \tag{20}$$

It can be shown (see Refs. [22,23,40]) that the calculation of these functional derivatives leads, respectively, to

$$\gamma = \mu_{n_0}+v(\boldsymbol{r})-v_{\rm el}(\boldsymbol{r})+v_{\rm xc}(n(\boldsymbol{r})), \tag{21}$$

$$\int d^3r\left\{v_{\rm el}(r)\theta\left(r-R^{n_i}_{\rm WS}\right)\right\} = 0, \tag{22}$$

where we introduced the shorthand notation

$$v_{\rm el}(r) \equiv \frac{Z}{r}-\int d^3r'\left\{\frac{n(r')-n_0\theta\left(r'-R^{n_i}_{\rm WS}\right)}{|\boldsymbol{r}'-\boldsymbol{r}|}\right\}. \tag{23}$$

We immediately note that since the trial potential is assumed to be local and all the charges are screened, that is, $n(r\to\infty)=n_0$, it follows from Eq. (21) that

$$v(\boldsymbol{r}) = v_{\rm el}(\boldsymbol{r})-v_{\rm xc}(n(\boldsymbol{r}))+v_{\rm xc}(n_0) \tag{24}$$

and

$$\gamma = \mu_{n_0}+v_{\rm xc}(n_0). \tag{25}$$

Together with equations for the eigenstates and the expression of the electron density, namely

$$\tilde{H}|\varphi_j\rangle = E_j|\varphi_j\rangle;\ \tilde{H}|\varphi_{\mathbf{k},s}\rangle = E_k|\varphi_{\mathbf{k},s}\rangle, \tag{26}$$

$$n(r) = g_s\sum_j f^F_{n_0,T}(E_j)|\varphi_j(\boldsymbol{r})|^2 + g_s\sum\!\!\!\!\!\!\int\frac{d^3k}{(2\pi)^3}\left\{f^F_{n_0,T}(E_k)|\varphi_{\mathbf{k},s}(\boldsymbol{r})|^2\right\}, \tag{27}$$

Eq. (24) forms the usual self-consistent-field (SCF) set of equations.

The additional condition Eq. (22) that stems from the approach will be called the "variational condition."

We denote by

$$n_0^{\rm eq}(n_i,Z,T,e^2,m),\quad v^{\rm eq}(n_i,Z,T,e^2,m;\boldsymbol{r}) \tag{28}$$

the solution of the system of Eqs. (22), (23), (24), (26), and (27). We will use the index "eq" to denote values of functionals taken at that equilibrium, that is, at $n_0 = n_0^{\rm eq}(n_i,Z,T,e^2,m)$ and $v(\boldsymbol{r}) = v^{\rm eq}(n_i,Z,T,e^2,m;\boldsymbol{r})$.

In particular, we denote the equilibrium free-energy per ion by

$$F^{\rm eq}(n_i,Z,T,e^2,m) \equiv F\{n_0,v(\boldsymbol{r});n_i,Z,T,e^2,m\}|_{\rm eq}. \quad (29)$$

D. Pressure formula

The thermodynamic definition of the electron pressure is

$$P \equiv n_i^2 \frac{\partial F^{\rm eq}(n_i,Z,T,e^2,m)}{\partial n_i}. \quad (30)$$

Using the general relation of Eq. (A7) (see Appendix A), we get

$$P = n_i^2 \left.\frac{\delta\Omega}{\delta n_i}\right|_{\rm eq}. \quad (31)$$

It was shown in Refs. [22,23,40] that Eq. (30) leads to

$$\begin{aligned} P = &-f_0^0(n_0,T) + n_0\mu_{n_0} - f_{\rm xc}(n_0,T,e^2,m) \\ &+ n_0 v_{\rm xc}(n_0) + n_0 v_{\rm el}\left(R_{\rm WS}^{n_i}\right)\big|_{\rm eq}, \end{aligned} \quad (32)$$

where $f_0^0(n_0,T,m)$ is the kinetic-entropic part of the free-energy density of a uniform electron gas having density n_0,

$$f_0^0(n_0,T,m) = g_s \sum\!\!\!\!\!\!\int \frac{d^3k}{(2\pi)^3}\left\{f^F_{n_0,T}(E_k)E_k - TS_{n_0,T}(E_k)\right\}, \quad (33)$$

$$f_0(n_0,T,e^2,m) = f_0^0(n_0,T) + f_{\rm xc}(n_0,T,e^2,m). \quad (34)$$

III. NUMERICAL METHODS AND DESCRIPTION OF THE VAAQP CODE

In the quantum cases, all wave functions needed to obtain the electron density are calculated by direct numerical integration of the radial wave equations using the Numerov scheme. Bound-state eigenvalues are found using a phase method similar to the one described in Ref. [41]. This method leads generally to a very fast convergence. Continuum-state contributions to observables are computed using an adaptive mesh refinement (AMR). In this way, even the contributions from narrow resonances in the continuum can be precisely taken into account, leading to observables that remain continuous in the case of pressure ionization (see, for instance, Ref. [42]).

The main objective of the VAAQP code is numerical calculations of plasma thermodynamics on the basis of the variational model described in Sec. II. The program is built as a C++ object-oriented code. In this way, a relative flexibility is obtained in the use and in the adaptation of the code to calculations based on different models. The calculations are organized as follows. The code can find solutions of the SCF equations with a fixed value of n_0, that is, to the system of Eqs. (23), (24), (26), and (27). The program looks for the solution corresponding to such an n_0 that the additional condition [Eq. (22)] is fulfilled.

Three options are available concerning the calculation of the electron density. The first one makes use of the nonrelativistic quantum formalism. In this case, all wave functions are computed by solving the Schrödinger equation. The second option is based on the relativistic quantum formalism. All bispinors are then computed by solving the Dirac equation. A third option allows us to calculate the density in the TF formalism. In each of these three cases, we apply the DFT in the framework of the LDA for the exchange-correlation term.

Several exchange-correlation terms are available in the literature. We have tried the Kohn-Sham exchange term (cf. Ref. [34]) with or without the Hedin-Lundqvist correlation term (cf. Ref. [43]), Perrot's term of Ref. [44], as well as the Iyetomi-Ichimaru term (cf. Refs. [39,45]). As concerns the WDM region (with a typical compression ratio of 1/2 to 10, and temperatures between a few electron volts and a few tens of electron volts), we found that results obtained using those different exchange-correlation terms were close to each other.

The Poisson equation (23) transformed into its differential form is solved using the standard Poisson-Helmholtz method (see, for instance, Refs. [46–48]).

To compare our variational approach to other models, the VAAQP code was equipped with various additional options allowing us to perform calculations based on approaches that are different from the variational one. These are a neutral WS sphere atom-in-jellium model (NWS option) and an INFERNO-type model (INFERNO option).

Each of these options was developed for a specific purpose. The INFERNO option allows us to apply the INFERNO model in a numerical implementation that is strictly identical to the one used in our variational option. Lets us recall that in the INFERNO-type model, the Friedel oscillations of the density are neglected, the potential is set to zero beyond the WS radius, and the WS sphere is neutral.

The interest of the NWS option is of a theoretical nature. Such a model does not exist in the literature: it is an atom-in-jellium model with the neutrality of the WS sphere imposed. When using this option, we solve Eqs. (23), (24), (26), and (27) together with the condition

$$Z - \int d^3r\left\{n(\boldsymbol{r})(1-\theta\left(r - R_{\rm WS}^{n_i}\right)\right\} = 0 \quad (35)$$

instead of the variational condition of Eq. (22). Comparisons with this model appear useful from a theoretical point of view, as an intermediate stage of comparison between the variational model and the well-known INFERNO model. In particular, it allows us to distinguish the respective effects of the two main hypotheses of the INFERNO model: neutrality of the WS sphere and zero potential outside the WS sphere.

Purely sequential calculation of a density-temperature point of the EOS can be made with VAAQP in a few minutes using a typical workstation (AMD Opteron 2384, Intel Xeon 5150). To reduce the execution time, the code was also equipped with a shared-memory parallel execution mode.

We paid particular attention to the precision of the calculations of the thermodynamic quantities. Indeed, the calculation of the virial pressure (see Sec. VI for more details) involves a subtraction between two energy values of the order of 10 hartree a_0^{-3}, whereas the obtained pressure values are of the order of 10^{-2} hartree a_0^{-3} with, in the worst cases, a precision of three digits. Typically, such a calculation requires a precision in the energies of the order of six digits.

In the case of the variational model, a valuable test for the code has been agreement between the results stemming from the three expressions for the electron pressure

(see Sec. VI). Such tests of thermodynamic consistency have been performed systematically in our calculations of EOS's and became a valuable criterion that allowed us to detect possible errors in numerical computation.

IV. EOS AND EXTENSIVE CHECK OF THERMODYNAMIC CONSISTENCY

In the case of the variational model, Eq. (32) means that the electron pressure is directly connected to the mean ionization value Z^* defined as follows:

$$Z^* \equiv \frac{n_0}{n_i}, \tag{36}$$

where n_0 is the asymptotic value of the electron density. Also in the literature, the dependence of Z^* on mass density ρ and temperature T is often considered as practically equivalent to the pressure values as a function of these parameters.

Although the study of the mean ionization appears to be useful to understand the differences of behavior between models, it raises problems of rigorous definition of Z^*. Indeed, Eq. (36) is not the only one definition of Z^* that can be used. A common way of defining the mean ionization is to subtract the number of bound electrons from the charge of the nucleus,

$$Z^* \equiv Z - \sum_{\ell} 2(2\ell+1) f^F\left(E_{n_r,\ell}\right). \tag{37}$$

This definition implies a distinction between bound and continuum states, and obviously such defined Z^* does not correspond to any well-defined observable in the sense of quantum mechanics. Another definition that may be justified by an analogy with the TF model makes use of the ratio of the electron density at the boundary of the WS sphere to the ion density,

$$Z^* \equiv n\left(R_{\mathrm{WS}}^{n_i}\right)/n_i. \tag{38}$$

Among the preceding definitions, none seems obvious to connect to the densities of charge carriers as defined in theories of conductivity or stemming from measurements. This problem was addressed, for example, in Ref. [49].

The definition of Z^* we use is Eq. (36), which corresponds to the apparent charge of the spread-out ions. The value of Z^* is then directly connected to the chemical potential μ_{n_0} [see Eq. (11)]. In fact, it also depends on the energy definition, or more precisely on the assumed value of the electrostatic potential at infinity. This is due to the fact that the invariant quantity in the problem is the electrochemical potential. Let us notice that the definition of Eq. (36), which is natural in all kinds of atom-in-jellium models, differs from Eq. (38). The latter appears as natural in INFERNO-type models where the potential is set to zero outside the WS sphere. In the case of the TF approximation to the electron density, the INFERNO model becomes identical to the usual TF ion-in-cell model. It was shown in Refs. [23,40] that this is also the case for the variational model. In the case of the TF electron density, Eqs. (36) and (38) thus lead to identical values of Z^*. Within the framework of the quantum INFERNO model, n_0 does not correspond, strictly speaking, to an asymptotic electron density value. Therefore, comparing nonobservable quantities obtained within such an atom-in-cell model to quantities obtained using "infinite" (that is, screened but considered in the whole space) models is a difficult task.

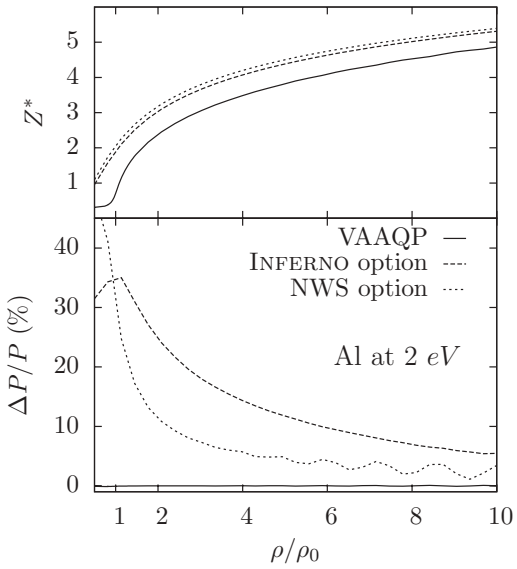

FIG. 1. Thermodynamic consistency of the different models along the aluminum 2-eV isotherm. Relative difference between thermodynamic and virial electron pressures is plotted vs the compression ratio (we use $\rho_0 = 2.7\ \mathrm{g\,cm^{-3}}$).

In the upper part of Fig. 1 are displayed the mean ionizations [in the sense of Eq. (36)] stemming from the three options of the VAAQP code, that is, variational, NWS, and INFERNO in the case of the aluminum 2-eV isotherm. As concerns the INFERNO model, we define n_0 (and thus Z^*) as the density associated with the electron chemical potential μ_{n_0} via Eq. (11). In the case of this isotherm, the variational model leads to results that differ significantly from the two others models. We recall that, in principle, it is not fully rigorous to compare the mean ionizations stemming from the INFERNO model to those stemming from the two atom-in-jellium models. However, as can be seen in the figure, the behaviors of the mean ionizations stemming from the NWS and INFERNO options appear qualitatively similar. This suggests that the consequences of the INFERNO model hypotheses rely mainly on the WS sphere neutrality and not on the change of boundary condition. For that reason, comparing mean ionizations stemming from the INFERNO model to the ones stemming from atom-in-jellium models can be relevant, if done with care. Indeed, this intermediate stage of comparison was one of the main purposes of considering the NWS option.

Among the main results we obtained using the VAAQP code is the direct check of consistency of the thermodynamic quantities obtained in the framework of our variational model. In this model, the electron pressure can be calculated in three ways. First, this pressure can be calculated by application of the formula presented in Eq. (32). Second, it can be calculated by numerical differentiation of the free-energy along an isotherm, using a simple finite-difference scheme. Third, we can calculate the electron pressure by applying the virial theorem. This theorem allows one to calculate the electron pressure from a simple combination of the kinetic and interaction energy densities. The proof and detailed study of this theorem in both the nonrelativistic and relativistic versions of the model are developed in Sec. VI. The virial definitions of

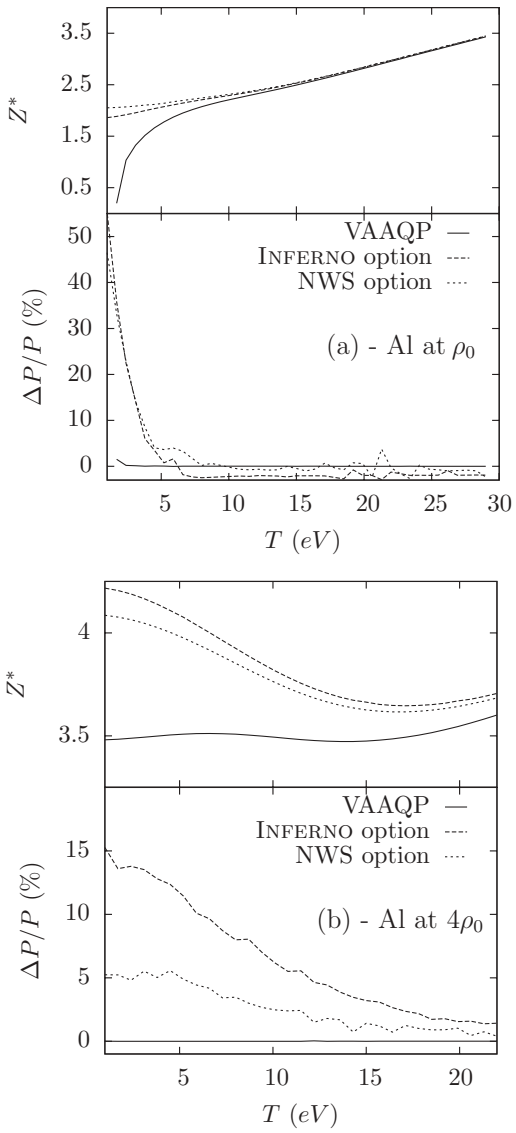

FIG. 2. Aluminum 2.7 g cm^{-3} (a) and 10.8 g cm^{-3} (b) isochoric curves (one time and four times solid density, respectively) for the three options of VAAQP.

the pressure are, respectively, those of Eqs. (55) and (81). In the case of the INFERNO model, no analytical pressure formula analogous to our Eq. (32) can be obtained, so in the case of that model, the use of such a formula is, in principle, unjustified.

In Fig. 1, a comparative illustration is presented of the thermodynamic consistency obtained with VAAQP on the 2-eV isotherm of aluminum. In the lower part of the figure, the relative difference between the thermodynamic and the virial pressures is displayed as a function of the compression ratio for the three options: variational (denoted by VAAQP), NWS, and INFERNO. As can be seen in the figure in the case of the variational calculations, all definitions of the pressure yield identical results all along the isotherm. As concerns the two other models, there is a disagreement of the order of tens of percent. In this case of relatively low temperature, the requirement of the WS sphere neutrality, with or without taking into account the Friedel oscillations, leads to a significant violation of the thermodynamic consistency.

As can be seen in the upper part of the figure, differences between the variational model and the two models using a neutral WS sphere remain in the high-density regime.

Figures 2(a) and 2(b) present a comparative picture of the thermodynamic consistency obtained with VAAQP on the 2.7 and 10.8 g cm^{-3} isochoric curves of aluminum, respectively, which correspond to solid density and four times solid density, respectively. It can be seen in these figures that, as temperature increases, both the INFERNO model and the NWS atom-in-jellium model become thermodynamically consistent in practice (see the relative electron pressure differences) and close to the variational model (see the mean ionization). When temperature increases, the electron density becomes uniform outside the WS sphere, and this way, the INFERNO model and the NWS atom-in-jellium model both appear to be good approximations to the variational model.

As may be seen by comparing Figs. 2(a) and 2(b), the higher the matter density is, the broader is the temperature region in which these models encounter thermodynamic consistency problems. There are two reasons for that: (a) increased matter density also means increased jellium density n_0 and increased Friedel oscillations decay length; (b) at high matter density, bound states or resonances may make a significant contribution to the electron density at the WS radius.

The linear-response theory of dense plasmas near zero temperature (see, for instance, [50]) can give a rough idea of the Friedel oscillations decay. Namely, the following behavior stems from the theory:

$$n(r) \sim r^{-3} e^{-2b_0 r} \sin(2a_0 r), \tag{39}$$

where a_0, b_0 are the real and imaginary parts of the zeroth-order pole of the Fermi-Dirac distribution, namely, in atomic units,

$$b_0 = \sqrt{-\mu_{n_0} + \sqrt{\mu_{n_0}^2 + \pi^2 T^2}}, \tag{40}$$

$$a_0 = \sqrt{+\mu_{n_0} + \sqrt{\mu_{n_0}^2 + \pi^2 T^2}}, \tag{41}$$

where we recall that μ_{n_0} is the chemical potential. For illustration, the $2b_0 R_{\rm WS}$ parameter, which is related to the magnitude of the Friedel oscillations at the WS radius, was calculated from VAAQP results on the aluminum EOS. Values of $2b_0 R_{\rm WS}$ as a function of compression ratio and temperature are displayed in Fig. 3. This picture should give

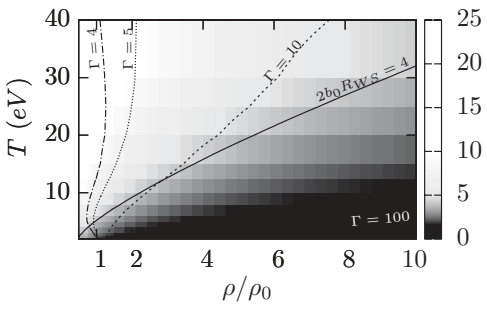

FIG. 3. Value of $2b_0 R_{\rm WS}$ found with VAAQP for aluminum as a function of compression ratio and temperature (we use $\rho_0 =$ 2.7 g cm^{-3}). The $2b_0 R_{\rm WS} = 4$ isoline is displayed in black on the figure as well as some Γ isolines.

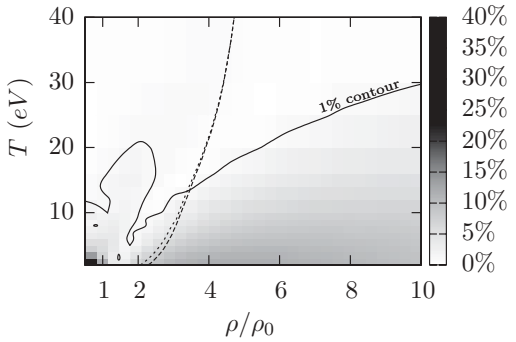

FIG. 4. Thermodynamic consistency of the INFERNO option. The relative difference between thermodynamic and virial electron pressures is displayed as a function of compression ratio and temperature in the case of aluminum (we use $\rho_0 = 2.7\ \mathrm{g\,cm^{-3}}$). The black line is the contour of the >1% region. The two dashed curves correspond to the Hugoniot shock adiabats obtained using, respectively, the thermodynamic (for the lower curve) and the virial (for the upper curve) definition of the pressure with the INFERNO option.

some indications of the region in which nonvariational models will not constitute a good approximation to the variational model, that is, the region in which they may lead to a significant violation of thermodynamic consistency. Some lines of constant Γ values are also displayed in this figure to give some idea of the validity domain of all models considered in this paper.

As was shown in the above paragraphs, the INFERNO model may be a good approximation to the variational model when the temperature is sufficiently high. A criterion we can propose with regard to thermodynamic consistency is the agreement between the virial pressure and the pressure stemming from Eq. (32), which becomes equivalent to the TF pressure formula when applied to the INFERNO model [$v_{\mathrm{el}}(R_{\mathrm{WS}}^{ni}) = 0$]. Figure 4 presents the relative difference between these two quantities as a function of compression ratio and temperature. The 1% contour plotted in the figure may give a rough idea of the domain of validity of the INFERNO approach with regard to thermodynamic consistency.

Let us notice that the region in which thermodynamic inconsistencies exceed 1% shows some qualitative similarity with the region of Fig. 3 in which $2b_0 R_{\mathrm{WS}} < 4$.

The temperature versus compression projections of the INFERNO option Hugoniot shock adiabats are also plotted in this figure. The two curves correspond, respectively, to the thermodynamic and to the virial definition of the electron pressure. As can be seen in this figure, these two curves depart significantly from one other outside the domain of thermodynamic consistency of the model.

Figure 5 presents the mean ionizations obtained in the case of aluminum using (a) the variational model (main option of VAAQP) [Fig. 5(a)], (b) the INFERNO option [Fig. 5(b)], and (c) the TFD model (TF option of VAAQP) [Fig. 5(c)]. In a similar way, Figs. 6, 7, and 8 present the mean ionizations obtained with these various models in the respective cases of iron, copper, and lead. The quantum calculations were made using the nonrelativistic option for the electron density. In all cases, the Kohn-Sham exchange term was used. As concerns

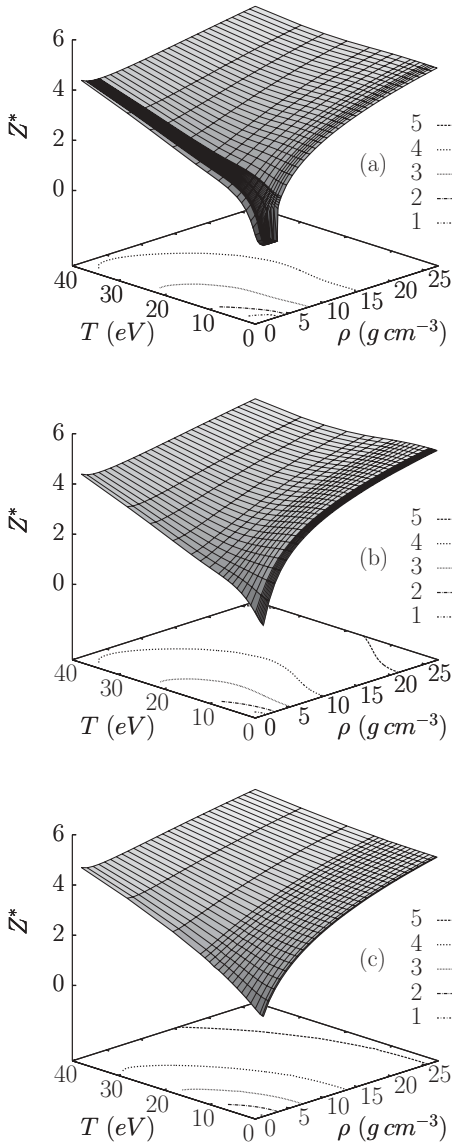

FIG. 5. Aluminum mean ionization obtained with VAAQP, INFERNO option, and TFD.

the temperature regime of interest in this study, the relativistic effects remain negligible even for heavy elements. The effects of a relativistic treatment on the 30-eV isotherm of ytterbium is shown in Appendix G, in Fig. 14. As can be viewed in this figure, the relative differences in the electron pressures and mean ionizations are less than 1% in the region of interest.

First, it can be seen that both thermal and pressure ionization phenomena are qualitatively reproduced by each of the three models. In general, using the quantum models we obtain lower mean ionizations than those stemming from the TFD model. This seems to be mainly due to the absence of shell structure in this latter model. As was mentioned earlier, the differences between the electron pressures obtained with the INFERNO model and those stemming from the TFD model strongly depend on the chosen pressure definition (thermodynamic or virial pressure). Indeed, even the sign of this difference can change.

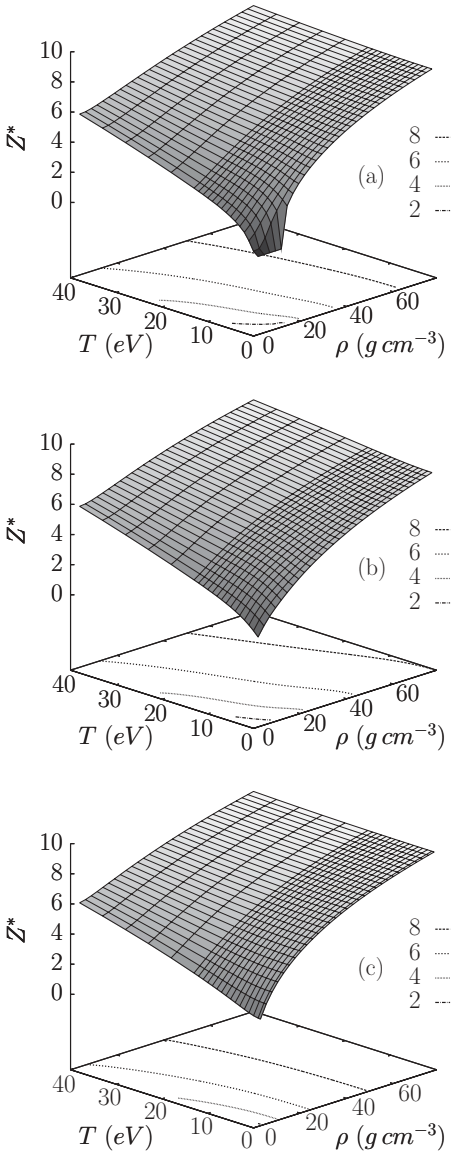

FIG. 6. Iron mean ionization obtained with VAAQP, INFERNO option, and TFD.

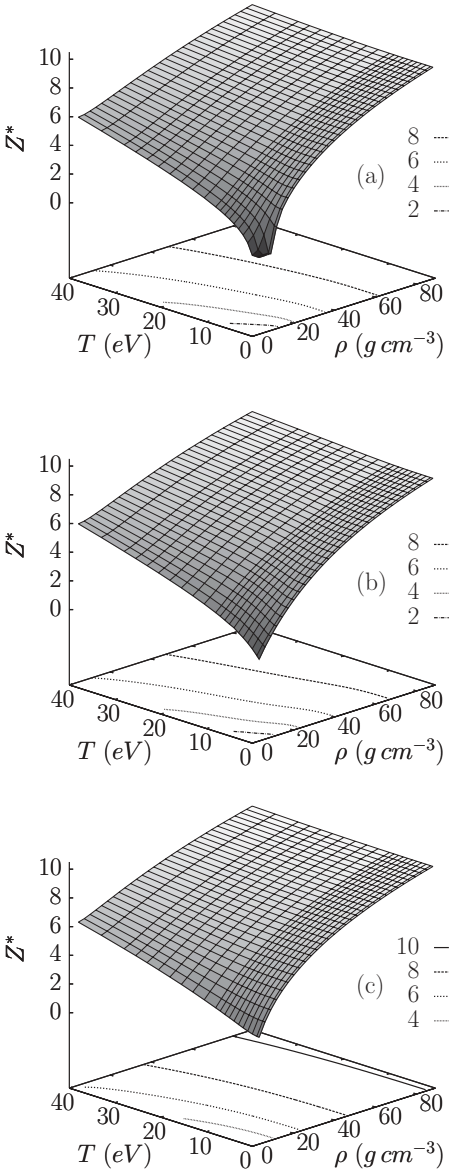

FIG. 7. Copper mean ionization obtained with VAAQP, INFERNO option, and TFD.

In the high-temperatures region, considering moderate densities, results stemming from the variational model tend to those stemming from the INFERNO model. For example, in the case of iron at 3.9 g cm^{-3} matter density, 40-eV temperature, differences in the mean ionization as well as in the electron pressure between these models are of the order of 0.1%. This agreement results from the strong decay of the Friedel oscillations in this regime.

In the high-densities region, at moderate temperatures, Friedel oscillations are weakly damped and results obtained using the variational model depart strongly from those obtained using the INFERNO model or the TF model.

As concerns the ultrahigh densities (high-coupling regime), the validity of all those models might be questionable. First, we recall that in all these models, one makes the hypothesis of an ion-ion correlation function in the form of a Heaviside function, which is only relevant in the case of moderate coupling. In addition, for coupling parameter of about $\Gamma \gtrsim 150$, a crystallization of the plasma is likely to occur (see, for example, Ref. [51]). Atom-in-jellium models are based on the calculation of a local potential around a single center. Periodic potentials typical of solid-state physics are intrinsically outside the possibility of such models. Thus, despite their improved thermodynamic consistency, the results stemming from the variational model in the region of high coupling, and in particular with regard to the cold compression path, are to be taken with care. However, in the variational model, the thermodynamic consistency is preserved even in the high-coupling region. This may constitute a strong point for the extension of the model to a wider validity domain, which may still exclude the solid-state regime.

Close to normal conditions, we obtain a finite ionization using either INFERNO or the TFD model [cf. Figs. 5–8(c)]. Such a behavior is related to the neutrality of the WS sphere, which appears naturally in the TF model and as a hypothesis in the

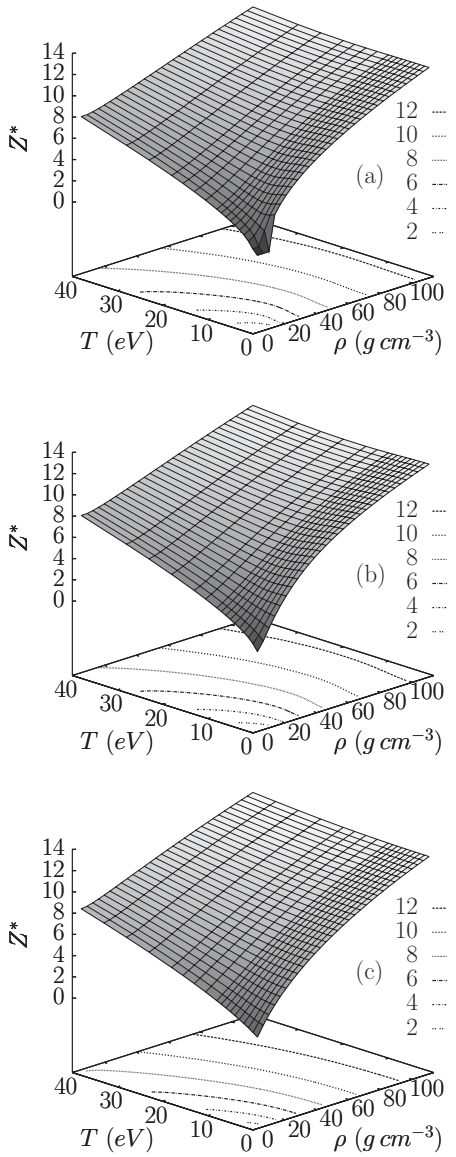

FIG. 8. Lead mean ionization obtained with VAAQP, INFERNO option, and TFD.

INFERNO model. In the case of the atom-in-jellium model with a neutral WS sphere, a similar behavior is observed. However, it is worth stressing that neither the INFERNO model nor the neutral WS sphere atom-in-jellium model are consistent in the sense of thermodynamics in this region.

As can be seen in Figs. 5–8(a), the solution of the variational model tends to the case of a quasineutral atom (mean ionization close to zero) in the vicinity of the normal conditions. In fact, the variational condition allows the electrostatic potential to extend beyond the WS sphere. In the TF case, the quasiclassical aspect of the model does not allow the existence of bound states and also results in the neutrality of the WS sphere. As mentioned in the previous paragraph, this leads to a finite mean ionization. However, with regard to the quantum cases, the extension of the potential beyond the WS sphere allows the existence of bound states that a neutral WS sphere condition would have forbidden (see, for example, Figs. 1 and 4 of Ref. [25]). At low temperatures, we can have a quasineutral atom solution of the SCF equations, that is, a solution with a number of bound electrons close to Z and a negligible contribution of the continuum, due to the low-temperature behavior of the Fermi-Dirac distribution. An upper bound of the matter density then exists, such that the corresponding WS radius is large enough to have $v_{\rm el}(r > R_{\rm WS}^{n_i}) \approx 0$. For matter densities below this bound, the quasineutral atom nearly fulfills the variational condition and may appear as an approximate solution of the variational model. These densities are usually of the order of $\rho_0/100$ and below.

However, it seems that a region of higher density exists (often extending slightly beyond ρ_0), where the mean ionization stemming from the variational calculations remains very low and where the quasineutral atom still constitutes an acceptable approximation to the variational solution. Moreover, as long as the mean ionization remains close to zero, the electronic pressure remains negligible and the free-energy remains almost constant with matter density.

This transition to the quasineutral atom in the vicinity of the normal conditions could indicate that the single-center model (in the sense of the cluster expansion) seems not to be valid in this region. This would mean that finite ionization at normal conditions may only be described by taking into account multicenter (molecular) effects that are disregarded in average-atom models.

V. HUGONIOT SHOCK ADIABATS OF ALUMINUM, IRON, COPPER, AND LEAD

To perform comparisons of our model with experimental data, the best quantities to choose are those that can be directly computed using the model and measured in experiments. Moreover, it would be appreciable that the experiments reach some regimes in which those quantities allow a clear discrimination among theories.

Average-atom models in themselves only give direct access to the thermodynamic quantities. For that reason, it is relevant to study the EOS measurements. As concerns the EOS of dense plasmas, only some particular thermodynamic paths can be reached in experiments. Among these, we can cite (a) the 0 K isothermal compression, as studied, for example, in diamond-anvil-cell experiments (see Ref. [52]); (b) isochoric heating,

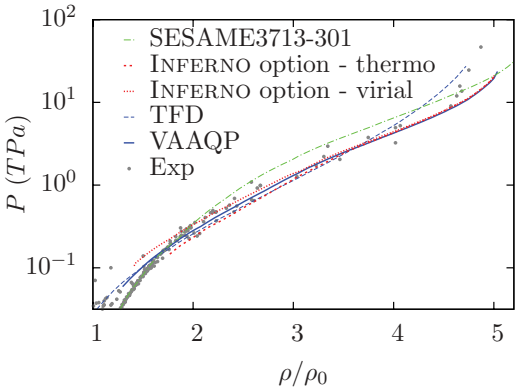

FIG. 9. (Color online) Aluminum principal Hugoniot shock adiabat obtained using VAAQP, INFERNO option, TFD, and the SESAME3713 table. We use $\rho_0 = 2.7\ \mathrm{g\,cm^{-3}}$.

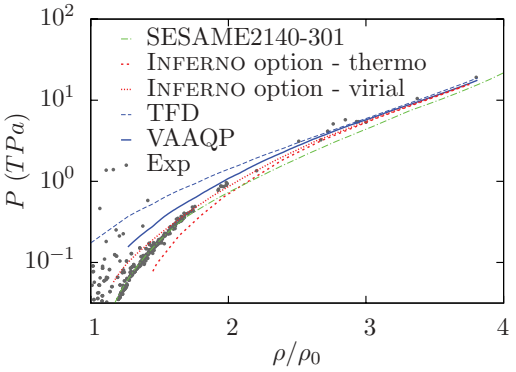

FIG. 10. (Color online) Iron principal Hugoniot shock adiabat obtained using VAAQP, INFERNO option, TFD, and the SESAME2140 table. We use $\rho_0 = 7.874\ \mathrm{g\,cm^{-3}}$.

as studied, for example, in Refs. [53–56]; and (c) Hugoniot adiabatic compression, as studied in shock wave compression experiments (see the "rusbank" database [57]).

In this section, we are interested in the Hugoniot adiabatic compression. It allows one to probe relatively high densities (typically between one and six times solid density) at relatively low temperatures (starting from the normal conditions, five times solid density is usually achieved at a temperature of the order of 100 eV). Among the main problems raised by the comparison to the Hugoniot shock adiabats are (a) the need to calculate EOS data at normal conditions, which usually lie outside the validity domain of the models hypotheses; and (b) the lack of temperature measurements that are needed to fully characterize the EOS point. Usually, measures made in shock wave compression experiments only lead to some bidimensional projection of the curve, which is intended to give the (ρ, P) projection after some calculations.

We present in Figs. 9, 10, 11, and 12 the principal Hugoniot shock adiabats for aluminum, iron, copper, and lead. These were obtained using, respectively, VAAQP, its INFERNO option with the two definitions of the pressure, its TFD option, and the SESAME 301-type EOS tables (see, for example, Ref. [58]). The experimental data are taken from the "rusbank" database [57].

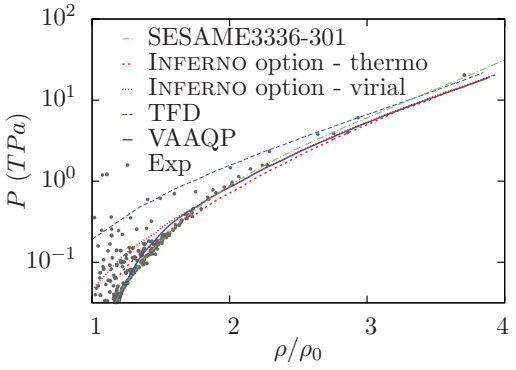

FIG. 11. (Color online) Copper principal Hugoniot shock adiabat obtained using VAAQP, INFERNO option, TFD, and the SESAME3336 table. We use $\rho_0 = 8.92\ \mathrm{g\,cm^{-3}}$.

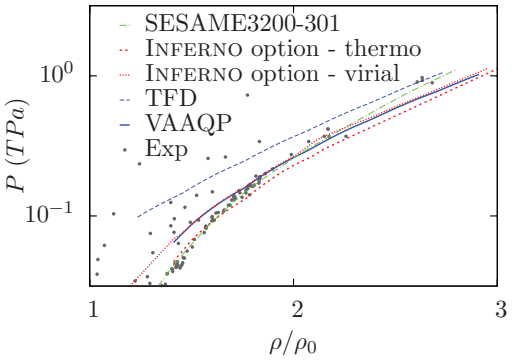

FIG. 12. (Color online) Lead principal Hugoniot shock adiabat obtained using VAAQP, INFERNO option, TFD, and the SESAME3200 table. We use $\rho_0 = 11.34\ \mathrm{g\,cm^{-3}}$.

Like many others, the SESAME 301-type EOS tables are made by the addition of three terms: an electron contribution (304-type table), an ion contribution (305-type table), and a cold-curve contribution (306-type table). It is worth stressing that the theoretical framework of such a subdivision is not clearly defined. Moreover, depending on the cold-curve contribution that is added, the process of shifting the total pressure to fit this cold curve may lead to severe consequences on the EOS. Nonetheless, the use of augmented-plane-wave (see Ref. [59]) or semiempirical (see, for example, Ref. [60]) cold-curve contributions ensures that the values along the cold region of the Hugoniot shock adiabat are very realistic.

The VAAQP code and all its options are designed to compute electron contributions to the thermodynamic quantities. To obtain total quantities and calculate the Hugoniot shock adiabats, we need to add an ion contribution to the pressure and internal energy. With regard to this ion contribution, we have chosen Hansen's formula of Ref. [61], which was used, for example, in Refs. [62,63]. Namely, we use Eqs. (6.90) and (6.91) of Ref. [41]. Figures 9, 10, 11, and 12 give an idea of the quality of the results stemming directly from the models. For that reason, we do not shift the results to fit a cold curve. Models of dense plasmas are generally intended to describe the matter at finite temperature. Disagreement in

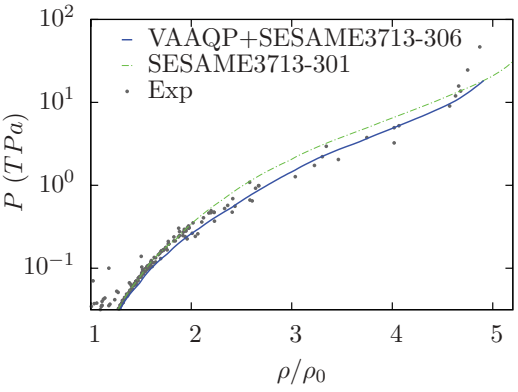

FIG. 13. (Color online) Aluminum principal Hugoniot shock adiabat obtained using VAAQP with the SESAME3713-306 cold-curve contribution. We use $\rho_0 = 2.7\ \mathrm{g\,cm^{-3}}$.

the low-pressure region is then to be expected, especially in the case of single-center models such as VAAQP or INFERNO. Nevertheless, we give as an example in Fig. 13 the aluminum shock adiabat obtained using VAAQP with Hansen's ion contribution and the SESAME 3713-306 cold-curve contribution. As can be seen, good agreement with the experiment is then achieved even in the low-pressures region.

VI. OTHER THERMODYNAMIC QUANTITIES AND VIRIAL THEOREM IN THE CASE OF VAAQP

As is well known, the virial theorem is fulfilled in the cases of classical (see Ref. [64]) and quantum (see Ref. [65]) exact many-body problems. The model we consider here is an approximation based on the mean-field idea, as are all average-atom models in general. For that reason, such models may not fulfill the virial theorem. Among the main advantages of the variational approach of the present paper is that it fulfills the virial theorem. This was not the case for all quantum models of the atom in plasma that have been proposed hitherto (see Sec. I).

In the case of the nonrelativistic TF model, Feynman *et al.* gave in Ref. [14] a proof of the virial theorem based on similarity considerations. In the case of our variational model, a formal generalization of this proof in the framework of the nonrelativistic quantum case is sketched in Ref. [22].

We give here a direct proof of the virial theorems in the cases of the nonrelativistic and relativistic versions of the variational model. This proof holds for any LDA exchange-correlation term. We think that the direct proof of these theorems offers a new point of view on the model and a better understanding of the thermodynamic inconsistencies of the other quantum models.

A. Internal energy

We can calculate the internal energy per ion from its usual thermodynamic definition:

$$U^{\mathrm{eq}}(n_i,Z,T,e^2,m) \equiv F^{\mathrm{eq}} - T\frac{\partial F^{\mathrm{eq}}}{\partial T}. \tag{42}$$

To calculate the derivative of the equilibrium free-energy per ion, we apply here the same general relation Eq. (A7) (see Appendix A) as for the pressure formula,

$$\frac{\partial F^{\mathrm{eq}}}{\partial T} = \left.\frac{\delta\Omega}{\delta T}\right|_{\mathrm{eq}}. \tag{43}$$

As is shown in Appendix A 2 [see Eqs. (A7)–(A17)], we obtain for the internal energy per ion the following quantum-mechanical expression:

$$U^{\mathrm{eq}}(n_i,Z,T,e^2) = U\{n_0,v(\boldsymbol{r});n_i,Z,T,e^2,m\}|_{\mathrm{eq}}, \tag{44}$$

where the functional on the right-hand side is defined as

$$\begin{aligned} U = {} & \frac{1}{n_i}\left(u_0^0(n_0,T,m) + u_{\mathrm{xc}}(n_0,T,e^2,m)\right) \\ & + \Delta U_1^0\{n_0,v(\boldsymbol{r});T,m\} \\ & + \Delta F_1^{\mathrm{el}}\{n_0,v(\boldsymbol{r});n_i,Z,T,e^2,m\} \\ & + \Delta U_1^{\mathrm{xc}}\{n_0,v(\boldsymbol{r});T,e^2,m\} \end{aligned} \tag{45}$$

with

$$u_0^0(n,T,m) \equiv g_s \iint \frac{d^3k}{(2\pi)^3}\left\{f^F_{n_0,T}(E_k)E_k\right\}, \tag{46}$$

$$u_{\mathrm{xc}}(n,T,e^2,m) \equiv f_{\mathrm{xc}}(n,T,e^2,m) - T\frac{\partial f_{\mathrm{xc}}(n,T,e^2,m)}{\partial T}, \tag{47}$$

$$\begin{aligned} \Delta U_1^0 = {} & g_s \sum_j f^F_{n_0,T}(E_j)\langle\varphi_j|\tilde{H}^0|\varphi_j\rangle \\ & + g_s \iint \frac{d^3k}{(2\pi)^3}\left\{f^F_{n_0,T}(E_k)\left(\langle\varphi_{\mathbf{k},s}|\tilde{H}^0|\varphi_{\mathbf{k},s}\rangle\right.\right. \\ & \left.\left. - \langle\varphi^0_{\mathbf{k},s}|\tilde{H}^0|\varphi^0_{\mathbf{k},s}\rangle\right)\right\}, \end{aligned} \tag{48}$$

$$\Delta U_1^{\mathrm{xc}} = \int d^3r\{u_{\mathrm{xc}}(n(\boldsymbol{r})) - u_{\mathrm{xc}}(n_0)\}. \tag{49}$$

B. Interaction energy

The thermodynamic definition of the interaction energy per ion can be obtained taking the derivative with respect to the squared electron charge e^2 (see Ref. [14]) (this was the reason for indicating explicitly this dependence in nearly all our formulas),

$$U^{\mathrm{int,eq}}(n_i,Z,T,e^2,m) \equiv e^2\frac{\partial F^{\mathrm{eq}}}{\partial(e^2)}. \tag{50}$$

Again, we use Eq. (A7) to calculate the derivative of the equilibrium free-energy per ion with respect to e^2,

$$\frac{\partial F^{\mathrm{eq}}}{\partial(e^2)} = \left.\frac{\delta\Omega}{\delta(e^2)}\right|_{\mathrm{eq}}. \tag{51}$$

As shown in Appendix A 3 [see steps leading to Eq. (A23)], we get

$$\begin{aligned} & U^{\mathrm{int,eq}}(n_i,Z,T,e^2,m) \\ & \quad = \left(u_{\mathrm{xc}}^{\mathrm{int}}(n_0,T,e^2,m) + \Delta F_1^{\mathrm{el}} + \Delta U_1^{\mathrm{xc,int}}\right)\Big|_{\mathrm{eq}}, \end{aligned} \tag{52}$$

where we have defined

$$u_{\mathrm{xc}}^{\mathrm{int}}(n,T,e^2,m) \equiv e^2\frac{\partial f_{\mathrm{xc}}(n,T,e^2,m)}{\partial(e^2)}, \tag{53}$$

$$\Delta U_1^{\mathrm{xc,int}} = \int d^3r\left\{u_{\mathrm{xc}}^{\mathrm{int}}(n(\boldsymbol{r})) - u_{\mathrm{xc}}^{\mathrm{int}}(n_0)\right\}. \tag{54}$$

C. Nonrelativistic virial theorem

Using the nonrelativistic virial theorem, we define the nonrelativistic virial electron pressure $P_{\rm vir}$ as follows:

$$P_{\rm vir} \equiv \frac{n_i}{3}(2U^{\rm eq} - U^{\rm int,eq}). \tag{55}$$

The virial theorem is fulfilled if $P = P_{\rm vir}$, where P is the electron pressure as defined by the thermodynamics [see Eq. (30)]. In terms of scaling laws, Eq. (55) is simply equivalent to

$$F^{\rm eq} = T\frac{\partial F^{\rm eq}}{\partial T} + \frac{1}{2}e^2\frac{\partial F^{\rm eq}}{\partial(e^2)} - \frac{3}{2}n_i\frac{\partial F^{\rm eq}}{\partial n_i}. \tag{56}$$

Using the expressions of U, $U^{\rm int}$ [see Eqs. (45) and (52)] in Eq. (55), we can write

$$\begin{aligned} P_{\rm vir} = {} & \frac{1}{3}\big(2u_0^0(n_0) + 2u_{\rm xc}(n_0) - u_{\rm xc}^{\rm int}(n_0)\big) \\ & + \frac{n_i}{3}\big(2\Delta U_1^0 + \Delta F_1^{\rm el} + 2\Delta U_1^{\rm xc} - \Delta U_1^{\rm xc,int}\big). \end{aligned} \tag{57}$$

Let us first consider the exchange-correlation part of Eq. (57). As is shown in Appendix F, if we assume that the whole dependence of $f_{\rm xc}$ on e^2 and m comes from the atomic units system, we have

$$\begin{aligned} & 2u_{\rm xc}(n,T,e^2,m) - u_{\rm xc}^{\rm int}(n,T,e^2,m) \\ & \quad = -3f_{\rm xc}(n,T,e^2,m) + 3n\frac{\partial f_{\rm xc}(n,T,e^2,m)}{\partial n}. \end{aligned} \tag{58}$$

The above relation can be applied directly to the zero-order contribution of Eq. (57), and also leads to the following relation for the first-order terms:

$$\begin{aligned} 2\Delta U_1^{\rm xc} - \Delta U_1^{\rm xc,int} = {} & -3\Delta F_1^{\rm xc} + 3\int d^3r\left\{\left(n\frac{\partial f_{\rm xc}(n)}{\partial n}\right)\Big|_{n=n(r)}\right. \\ & \left. - \left(n\frac{\partial f_{\rm xc}(n)}{\partial n}\right)\Big|_{n=n_0}\right\}. \end{aligned} \tag{59}$$

Using Eq. (D8) for the bound states and Eqs. (D8) and (D9) of Appendix D 1, integrating over the whole space and applying the Green theorem, we get

$$\begin{aligned} & \int d^3r\{(\boldsymbol{r}\cdot\boldsymbol{\nabla}v(\boldsymbol{r}))|\varphi_j(\boldsymbol{r})|^2\} \\ & \quad = -2\left(-\frac{\hbar^2}{2m}\right)\int d^3r\{\varphi_j^*(\boldsymbol{r})\nabla^2\varphi_j(\boldsymbol{r})\} \\ & \qquad - \frac{\hbar^2}{2m}\int_{\Sigma_\infty}\boldsymbol{dS}\cdot\{\varphi_j^*(\boldsymbol{r})\boldsymbol{\nabla}(\boldsymbol{r}\cdot\boldsymbol{\nabla}\varphi_j(\boldsymbol{r})) \\ & \qquad - (\boldsymbol{\nabla}\varphi_j^*(\boldsymbol{r}))(\boldsymbol{r}\cdot\boldsymbol{\nabla}\varphi_j(\boldsymbol{r}))\}, \end{aligned} \tag{60}$$

where the surface term is zero due to the exponential decay of the bound wave functions.

For the part involving the continuum and plane-wave states, we can use Eqs. (D8) and (D9) in the same fashion as before in order to write

$$\begin{aligned} & \int d^3r\{(\boldsymbol{r}\cdot\boldsymbol{\nabla}v(\boldsymbol{r}))|\varphi_{E,\ell,m}(\boldsymbol{r})|^2\} \\ & \quad = I_S - 2\left(-\frac{\hbar^2}{2m}\right)\int d^3r\big\{\varphi_{E,\ell,m}^*(\boldsymbol{r})\nabla^2\varphi_{E,\ell,m}(\boldsymbol{r}) \\ & \qquad - \varphi_{E,\ell,m}^{0*}(\boldsymbol{r})\nabla^2\varphi_{E,\ell,m}^0(\boldsymbol{r})\big\}, \end{aligned} \tag{61}$$

where the surface term I_S is

$$\begin{aligned} I_S = {} & -\frac{\hbar^2}{2m}\int_{\Sigma_\infty}\boldsymbol{dS}\cdot\big\{\varphi_{E,\ell,m}^*(\boldsymbol{r})\boldsymbol{\nabla}(\boldsymbol{r}\cdot\boldsymbol{\nabla}\varphi_{E,\ell,m}(\boldsymbol{r})) \\ & - (\boldsymbol{\nabla}\varphi_{E,\ell,m}^*(\boldsymbol{r}))(\boldsymbol{r}\cdot\boldsymbol{\nabla}\varphi_{E,\ell,m}(\boldsymbol{r})) \\ & - \varphi_{E,\ell,m}^{0*}(\boldsymbol{r})\boldsymbol{\nabla}\big(\boldsymbol{r}\cdot\boldsymbol{\nabla}\varphi_{E,\ell,m}^0(\boldsymbol{r})\big) \\ & + \big(\boldsymbol{\nabla}\varphi_{E,\ell,m}^{0*}(\boldsymbol{r})\big)\big(\boldsymbol{r}\cdot\boldsymbol{\nabla}\varphi_{E,\ell,m}^0(\boldsymbol{r})\big)\big\}. \end{aligned} \tag{62}$$

As is shown in Appendix E 1, this surface term vanishes if it is integrated over energy in the case of the system of an atom in the infinite jellium. This is closely related to the Friedel sum rule. Thus, summing Eq. (60) over the bound states and integrating Eq. (61) over the continuum, we get the relation

$$2\Delta U_1^0 = -\int d^3r\{n(\boldsymbol{r})\boldsymbol{r}\cdot\boldsymbol{\nabla}v(\boldsymbol{r})\} \equiv -I_{\rm vir}^{\rm nr}. \tag{63}$$

Let us define the following two quantities:

$$I_{\rm el} \equiv -\int d^3r\{n(\boldsymbol{r})\boldsymbol{r}\cdot\boldsymbol{\nabla}v_{\rm el}(\boldsymbol{r})\}, \tag{64}$$

$$I_{\rm xc} \equiv \int d^3r\{n(\boldsymbol{r})\boldsymbol{r}\cdot\boldsymbol{\nabla}(v_{\rm xc}(n(\boldsymbol{r})) - v_{\rm xc}(n_0))\}. \tag{65}$$

It is shown in Appendix B that

$$I_{\rm el} = -\Delta F_1^{\rm el} + 3\frac{n_0}{n_i}v_{\rm el}\big(R_{\rm WS}^{n_i}\big) + 3\int_{R_{\rm WS}^{n_i}}^{\infty}dr\{4\pi r^2 v_{\rm el}(r)\}, \tag{66}$$

and in Appendix C that

$$\begin{aligned} I_{\rm xc} = {} & 3\Delta F_1^{\rm xc} - 3\int d^3r\left\{\left(n\frac{\partial f_{\rm xc}(n)}{\partial n}\right)\Big|_{n=n(r)}\right. \\ & \left. - \left(n\frac{\partial f_{\rm xc}(n)}{\partial n}\right)\Big|_{n=n_0}\right\} \end{aligned} \tag{67}$$

$$= 2\Delta U_1^{\rm xc} - \Delta U_1^{\rm xc,int}. \tag{68}$$

Finally, we recall the well-known relation between the internal and free-energy densities of the nonrelativistic ideal electron gas,

$$\tfrac{2}{3}u_0^0(n_0) = -f_0^0(n_0) + n_0\mu_{n_0}. \tag{69}$$

As a consequence of Eqs. (63), (66), (68), and (69), we can write from Eq. (57)

$$\begin{aligned} P_{\rm vir} = {} & -f_0^0(n_0) + n_0\mu_{n_0} - f_{\rm xc}(n_0) + n_0 v_{\rm xc}(n_0) + n_0 v_{\rm el}\big(R_{\rm WS}^{n_i}\big) \\ & - \frac{1}{3}\big(I_{\rm vir}^{\rm nr} + I_{\rm el} + I_{\rm xc}\big) + \int_{R_{\rm WS}^{n_i}}^{\infty}dr\{4\pi r^2 v_{\rm el}(r)\}. \end{aligned} \tag{70}$$

We have obtained the following:

$$P_{\rm vir} = P \Leftrightarrow \frac{1}{3}\big(I_{\rm vir}^{\rm nr} + I_{\rm el} + I_{\rm xc}\big) = \int_{R_{\rm WS}^{n_i}}^{\infty}dr\{4\pi r^2 v_{\rm el}(r)\}. \tag{71}$$

Thus, a sufficient condition to fulfill the virial theorem is

$$v(r) = v_{\rm el}(r) - v_{\rm xc}(n(r)) + v_{\rm xc}(n_0), \qquad \int_{R_{\rm WS}^{n_i}}^{\infty} dr\{4\pi r^2 v_{\rm el}(r)\} = 0. \tag{72}$$

This sufficient condition is identical to the variational equations [Eqs. (22), (23), (24), (26), and (27)]. The previous derivation allows us to have a slightly different point of view on the model. Provided that we construct an atom-in-jellium model from heuristic consideration, building the internal and interaction energies from their quantum-mechanical expressions, then it is possible to get the variational condition as a consequence of the virial theorem in this model. Let us stress that the virial theorem is respected for any form of the local exchange-correlation free-energy density provided it does not depend on the squared electron charge other than via the atomic energy units present in the temperature and the electron density dependences.

D. $\boldsymbol{\alpha}\cdot\tilde{\mathbf{P}}$ energy (kinetic energy in the relativistic case)

A thermodynamic definition of the $\boldsymbol{\alpha}\cdot\tilde{\mathbf{P}}$ energy can be obtained by a variation of the electron mass m and of the squared electron charge e^2,

$$T^{\rm eq}(n_i,Z,T,e^2,m) \equiv F^{\rm eq} - T\frac{\partial F^{\rm eq}}{\partial T} - e^2\frac{\partial F^{\rm eq}}{\partial (e^2)} - m\frac{\partial F^{\rm eq}}{\partial m}. \tag{73}$$

As is shown in Appendix A 2, applications of Eq. (A7) to the derivative with respect to the temperature T and to the electron mass m, respectively, lead to Eqs. (A17) and (A21). We recall that

$$\tilde{T} = \boldsymbol{\alpha}\cdot\tilde{\mathbf{P}} = \tilde{H} - m\frac{\partial \tilde{H}}{\partial m}. \tag{74}$$

Thus, we obtain the following quantum-mechanical expression for the $\boldsymbol{\alpha}\cdot\tilde{\mathbf{P}}$ energy:

$$T^{\rm eq}(n_i,Z,T,e^2) = \mathcal{T}\{n_0,v(\boldsymbol{r});n_i,Z,T,e^2,m\}|_{\rm eq}, \tag{75}$$

where we defined the functional

$$\mathcal{T} = \frac{1}{n_i}\left(t_0^0(n_0,T,m) + t_{\rm xc}(n_0,T,e^2,m)\right) + \Delta T_1\{n_0,v(\boldsymbol{r});T,m\} + \Delta T_1^{\rm xc}\{n_0,v(\boldsymbol{r});T,e^2,m\} \tag{76}$$

with

$$t_0^0(n,T,m) \equiv u_0^0 + mc^2\, g_s \sum\!\!\!\!\!\!\int \frac{d^3k}{(2\pi)^3}\left\{f_{n_0,T}^F(E_k)\frac{E_k}{E_k+mc^2}\right\}, \tag{77}$$

$$t_{\rm xc}(n,T,e^2,m) \equiv f_{\rm xc}(n) - T\frac{\partial f_{\rm xc}(n)}{\partial T} - e^2\frac{\partial f_{\rm xc}(n)}{\partial (e^2)} - m\frac{\partial f_{\rm xc}(n)}{\partial m}, \tag{78}$$

$$\Delta T_1 = g_s\sum_j f_{n_0,T}^F(E_j)\langle\varphi_j|\tilde{T}|\varphi_j\rangle + g_s\sum\!\!\!\!\!\!\int \frac{d^3k}{(2\pi)^3}\left\{f_{n_0,T}^F(E_k)\left(\langle\varphi_{\mathbf{k},s}|\tilde{T}|\varphi_{\mathbf{k},s}\rangle - \langle\varphi_{\mathbf{k},s}^0|\tilde{T}|\varphi_{\mathbf{k},s}^0\rangle\right)\right\}, \tag{79}$$

$$\Delta T_1^{\rm xc} = \int d^3r\{t_{\rm xc}(n(\boldsymbol{r})) - t_{\rm xc}(n_0)\}. \tag{80}$$

E. Relativistic (general) virial theorem

We define the relativistic (or general) virial electron pressure $P_{\rm vir}$ as

$$P_{\rm vir} \equiv \frac{n_i}{3}(T^{\rm eq} + U^{\rm int,eq}). \tag{81}$$

Again, the virial theorem will be fulfilled if $P = P_{\rm vir}$, where P is given in Eq. (30). This is equivalent to

$$F^{\rm eq} = T\frac{\partial F^{\rm eq}}{\partial T} + m\frac{\partial F^{\rm eq}}{\partial m} - 3n_i\frac{\partial F^{\rm eq}}{\partial n_i}. \tag{82}$$

This relation could seem qualitatively different from the nonrelativistic one. In fact, what enters here is the $\boldsymbol{\alpha}\cdot\tilde{\boldsymbol{P}}$ energy density, which is equivalent to the difference between internal and interaction energy densities in the particular nonrelativistic case (and also in the ultrarelativistic case), whereas in the general case, it can only be obtained from the variation of the mass (or of the momentum).

Using the expressions of $\mathcal{T}$, $U^{\rm int}$ in Eq. (82), we can write

$$P_{\rm vir} = \frac{1}{3}\left(t_0^0(n_0) + t_{\rm xc}(n_0) + u_{\rm xc}^{\rm int}(n_0)\right) + \frac{n_i}{3}\left(\Delta T_1 + \Delta F_1^{\rm el} + \Delta T_1^{\rm xc} + \Delta U_1^{\rm xc,int}\right). \tag{83}$$

We first consider the exchange-correlation part of Eq. (83). It is shown in Appendix F that using the same procedure as in the nonrelativistic case, we get

$$t_{\rm xc}(n,T,e^2,m) + u_{\rm xc}^{\rm int}(n,T,e^2,m) = -3f_{\rm xc}(n,T,e^2,m) + 3n\frac{\partial f_{\rm xc}(n,T,e^2,m)}{\partial n}. \tag{84}$$

The above relation can be applied directly to the zero-order contribution of Eq. (83), and also leads to the following relation for the first-order terms:

$$\Delta T_1^{\rm xc} + \Delta U_1^{\rm xc,int} = -3\Delta F_1^{\rm xc} + 3\int d^3r\left\{\left(n\frac{\partial f_{\rm xc}(n)}{\partial n}\right)\Big|_{n=n(\boldsymbol{r})} - \left(n\frac{\partial f_{\rm xc}(n)}{\partial n}\right)\Big|_{n=n_0}\right\}. \tag{85}$$

We start now from Eqs. (D17) and (D18) (see Appendix D 2). Using Eq. (D17) for the bound states, integrating over the whole space, and applying the Green theorem, we get

$$\int d^3r\{(\boldsymbol{r}\cdot\nabla v(\boldsymbol{r}))|\varphi_j(\boldsymbol{r})|^2\} = -(-i\hbar c)\int d^3r\{\varphi_j^\dagger(\boldsymbol{r})\boldsymbol{\alpha}\cdot\nabla\varphi_j(\boldsymbol{r})\} - i\hbar c\int_{\Sigma_\infty}\boldsymbol{dS}\cdot\{(\varphi_j^\dagger(\boldsymbol{r})\boldsymbol{\alpha}(\boldsymbol{r}\cdot\nabla\varphi_j(\boldsymbol{r})))\}, \tag{86}$$

where the surface term is zero due to the exponential decay of the bound bispinors.

Now considering the continuum and plane-wave contribution, we can use Eqs. (D17) and (D18) in the same manner as above to write

$$\int d^3r\{(\boldsymbol{r}\cdot\boldsymbol{\nabla}v(\boldsymbol{r}))|\varphi_{E,\kappa,m}(\boldsymbol{r})|^2\} = I_S - (-i\hbar c)\int d^3r\big\{\varphi^{\dagger}_{E,\kappa,m}(\boldsymbol{r})\boldsymbol{\alpha}\cdot\boldsymbol{\nabla}\varphi_{E,\kappa,m}(\boldsymbol{r}) - \varphi^{0\,\dagger}_{E,\kappa,m}(\boldsymbol{r})\boldsymbol{\alpha}\cdot\boldsymbol{\nabla}\varphi^{0}_{E,\kappa,m}(\boldsymbol{r})\big\}, \tag{87}$$

where the surface term I_S is

$$I_S = -i\hbar c\int_{\Sigma_\infty}\boldsymbol{dS}\cdot\big\{\varphi^{\dagger}_{E,\kappa,m}(\boldsymbol{r})\boldsymbol{\alpha}(\boldsymbol{r}\cdot\boldsymbol{\nabla}\varphi_{E,\kappa,m}(\boldsymbol{r})) - \varphi^{0\,\dagger}_{E,\kappa,m}(\boldsymbol{r})\boldsymbol{\alpha}(\boldsymbol{r}\cdot\boldsymbol{\nabla}\varphi^{0}_{E,\kappa,m}(\boldsymbol{r}))\big\}. \tag{88}$$

As is shown in Appendix E 2, this surface term disappears after integration over energy in the case of an atom surrounded by an infinite jellium. Again, this is related to the Friedel sum rule. Thus, summing Eq. (86) over the bound states and integrating Eq. (87) over the continuum, we get the relation

$$\Delta T_1 = -\int d^3r\{n(\boldsymbol{r})\boldsymbol{r}\cdot\boldsymbol{\nabla}v(\boldsymbol{r})\} \equiv -I^R_{\rm vir}. \tag{89}$$

We recall the well-known relation in the relativistic case between $\boldsymbol{\alpha}\cdot\tilde{\boldsymbol{P}}$ and free-energy densities of the ideal electron gas,

$$\tfrac{1}{3}t^0_0(n_0) = -f^0_0(n_0) + n_0\mu_{n_0}. \tag{90}$$

Considering Eqs. (89), (66), (68), and (90), we can write from Eq. (83)

$$P_{\rm vir} = -f^0_0(n_0) + n_0\mu_{n_0} - f_{\rm xc}(n_0) + n_0 v_{\rm xc}(n_0) + n_0 v_{\rm el}\big(R^{n_i}_{\rm WS}\big) - \frac{1}{3}\big(I^R_{\rm vir} + I_{\rm el} + I_{\rm xc}\big) + \int_{R^{n_i}_{\rm WS}}^{\infty} dr\{4\pi r^2 v_{\rm el}(r)\}. \tag{91}$$

Again, we obtain that the sufficient condition in order to fulfill the virial theorem is Eq. (72) and that it corresponds exactly to the variational equations of the model.

This virial theorem obviously includes the nonrelativistic[1] result as a particular case implying $T^{\rm eq} = 2U^{\rm kin,eq}$, where $U^{\rm kin,eq} \equiv U^{\rm eq} - U^{\rm int,eq}$ is the kinetic energy of the system.

Remark. In fact, as we disregard the positon states of the Dirac equation in the calculation of the first-order contribution, it is not relevant to treat the zero-order contribution within the relativistic theory framework. If relativistic effects were to be relevant for the ideal electron gas, then disregarding positon states will not be fully justified. Indeed, in the VAAQP code, we always treat the zero-order contribution in the nonrelativistic approximation. For that reason, when performing relativistic calculations, we obviously apply the following modified definition of the virial electron pressure:

$$P_{\rm vir} = \frac{1}{3}\big(2u^0_0(n_0) + 2u_{\rm xc}(n_0) - u^{\rm int}_{\rm xc}(n_0)\big) + \frac{n_i}{3}\big(\Delta T_1 + \Delta F^{\rm el}_1 + \Delta T^{\rm xc}_1 + \Delta U^{\rm xc,int}_1\big). \tag{92}$$

VII. CONCLUSION

In this paper, the theory and results of the numerical code VAAQP are presented. The initial formalism of the variational model is extended to the relativistic case. Formulas for the main thermodynamic quantities, such as internal, interaction, and $\boldsymbol{\alpha}\cdot\tilde{\boldsymbol{P}}$ energies, are derived in their nonrelativistic and relativistic versions. Using these quantities, the respective virial theorems are proven. It is shown that this proof holds in both cases for all local-density-approximations (LDA's) to the exchange-correlation potential.

The numerical methods that are applied in the VAAQP code are described. These methods include an efficient solver of the Schrödinger and Dirac equations with an adaptive mesh refinement (AMR) for the continuum energy integrations. The self-consistent-field (SCF) equations in the framework of the atom-in-jellium model are solved using the Poisson-Helmholtz iterative method initially described in Refs. [46–48]. This code is designed to solve the equations of the variational model and is also equipped with options applying other approaches such as INFERNO within the same numerical implementation.

Equation-of-state (EOS) calculations are performed using VAAQP for aluminum, iron, copper, and lead in the warm-dense-matter (WDM) regime. Comparisons with the Thomas-Fermi-Dirac (TFD) and INFERNO models as well as with a neutral Wigner-Seitz (WS) sphere atom-in-jellium model are presented. Starting from the example of aluminum, a comparative study of the thermodynamic consistency of these different models is performed. This study relies on the relative difference between values stemming from the thermodynamic and the virial formulas for the electron pressure. In particular, a preliminary analysis of the validity domain of the INFERNO model is reported.

Comparisons of the results obtained using VAAQP and its various options on Hugoniot shock adiabats are compared with each other and to available experimental data gathered in Ref. [57]. Although this kind of comparison does not provide a clear way to discriminate among the models, it indicates that the variational model may be a promising theoretical tool for the description of dense plasmas in a part of the WDM regime.

The VAAQP model and code constitute a solution to the old problem of how to describe quantum plasmas within the single-center approach preserving thermodynamic consistency. The code is able to calculate thermodynamic properties of dense plasmas in a wide range of matter densities and temperatures. Results obtained in the framework of the present study raise once again the problem of the description of matter outside the moderate coupling region using a simplified single-center model. In particular, further improvement of the variational approach is probably possible and needed to access the normal condition domain. Among the possible improvements is the extension of the model toward more realistic approximations to the ion-ion correlations.

[1]Formally, it includes the ultrarelativistic result as well. However, as we disregard the negative energy states while using the Dirac equation, we choose not to mention the ultrarelativistic limit.

ACKNOWLEDGMENTS

The authors take pleasure in acknowledging very useful discussions with Bogdan Cichocki, especially on ion pressure corrections to the model, as well as with François Perrot on the AJCI model. The authors would like to thank Brian Wilson, Philip Sterne, and Stephen Libby for providing them with results from the PURGATORIO code to test the INFERNO option of the VAAQP code. They would also like to thank Scott Crockett for providing them with the SESAME equation-of-state database. Thanks are also due to Philippe Arnault, Christopher Bowen, Franck Gilleron, and Jean-Christophe Pain for their careful rereading of the manuscript, suggestions, and corrections. The authors are also grateful to Stéphane Bernard, Jean Bruneau, Gérard Dejonghe, Gérald Faussurier, Gilles Maynard, and Frank Rosmej for helpful discussions. The main part of this work has been performed at the CEA, IRAMIS and supported by the European Communities under the contract of association between EURATOM and CEA within the framework of the European Fusion Program.

APPENDIX A: THERMODYNAMIC QUANTITIES AND FUNCTIONAL DERIVATIVES

The functional derivatives of the free-energy density with respect to n_0, $v(\boldsymbol{r})$, n_i of the model were studied in Refs. [22,23,40]. We present here results for the functional derivatives of the free-energy density with respect to T, m, and e^2. These are useful in the derivation of all other thermodynamic quantities and of the virial theorems.

1. General relation

Let $F\{\overline{X},\overline{Y}\}$ be a functional of $\overline{X}=\{X_\alpha\}$ and $\overline{Y}=\{Y_\beta\}$. We call its dependences on the X_α "*internal*," and its dependences on the Y_β "*external*." We minimize F with respect to its internal (or $\overline{X}$) dependences with a number of additional constraints $\{C_j\{\overline{X},\overline{Y}\}=0\}$. We then define the functional $\Omega\{\overline{X},\overline{Y}\}$ as follows:

$$\Omega\{\overline{X},\overline{Y}\}\equiv F\{\overline{X},\overline{Y}\}-\sum_j \gamma_j C_j\{\overline{X},\overline{Y}\}, \tag{A1}$$

the $\{\gamma_j\}$ being Lagrange multipliers associated with the constraints. We have to fulfill

$$\frac{\delta\Omega\{\overline{X},\overline{Y}\}}{\delta X_\alpha}=\frac{\delta F\{\overline{X},\overline{Y}\}}{\delta X_\alpha}-\sum_j \gamma_j\frac{\delta C_j\{\overline{X},\overline{Y}\}}{\delta X_\alpha}=0. \tag{A2}$$

We denote by $\overline{X}^{\rm eq}\{\overline{Y}\}$ the solution of this system and define the functional

$$F^{\rm eq}\{\overline{Y}\}\equiv F\{\overline{X}^{\rm eq}\{\overline{Y}\},\overline{Y}\}. \tag{A3}$$

As concerns derivatives of $F^{\rm eq}$ with respect to any of the external dependences, we have the relation

$$\frac{\delta F^{\rm eq}\{\overline{Y}\}}{\delta Y_\beta}=\frac{\delta F\{\overline{X},\overline{Y}\}}{\delta Y_\beta}+\sum_\alpha \frac{\delta F\{\overline{X},\overline{Y}\}}{\delta X_\alpha}\bigg|_{\overline{X}=\overline{X}^{\rm eq}\{\overline{Y}\}}\frac{\delta X_\alpha^{\rm eq}\{\overline{Y}\}}{\delta Y_\beta}. \tag{A4}$$

As $\overline{X}^{\rm eq}\{\overline{Y}\}$ fulfills Eq. (A2),

$$\frac{\delta F^{\rm eq}\{\overline{Y}\}}{\delta Y_\beta}=\frac{\delta F\{\overline{X},\overline{Y}\}}{\delta Y_\beta}+\sum_{\alpha,j}\gamma_j\frac{\delta C_j\{\overline{X},\overline{Y}\}}{\delta X_\alpha}\bigg|_{\overline{X}=\overline{X}^{\rm eq}\{\overline{Y}\}}\frac{\delta X_\alpha^{\rm eq}\{\overline{Y}\}}{\delta Y_\beta} \tag{A5}$$

$$=\frac{\delta F\{\overline{X},\overline{Y}\}}{\delta Y_\beta}+\sum_j\gamma_j\left(\frac{\delta C_j\{\overline{X}^{\rm eq}\{\overline{Y}\},\overline{Y}\}}{\delta Y_\beta}-\frac{\delta C_j\{\overline{X},\overline{Y}\}}{\delta Y_\beta}\bigg|_{\overline{X}=\overline{X}^{\rm eq}\{\overline{Y}\}}\right). \tag{A6}$$

Recalling that $\overline{X}^{\rm eq}$ is such that the constraints are fulfilled, that is, $C_j\{\overline{X}^{\rm eq}\{\overline{Y}\},\overline{Y}\}=0$, we get

$$\frac{\delta F^{\rm eq}}{\delta Y_\beta}=\frac{\delta F}{\delta Y_\beta}-\sum_j\gamma_j\frac{\delta C_j}{\delta Y_\beta}\bigg|_{\overline{X}=\overline{X}^{\rm eq}}=\frac{\delta\Omega}{\delta Y_\beta}\bigg|_{\rm eq}. \tag{A7}$$

In particular, if the external dependences of F are local, then $F^{\rm eq}$ is a function and Eq. (A7) can be written with ∂ instead of δ on the left-hand side. In the case of our free-energy density, the internal dependences are on n_0, $v(\boldsymbol{r})$, whereas dependences on n_i, Z, T, e^2, and m are to be considered as external.

2. Case of m,T

In the case of a variable $\xi\in\{T,m\}$, that is, of an external dependence of the electron density functional [denoted by $n(\boldsymbol{r})$], we can write

$$\frac{\partial F^{\rm eq}}{\partial\xi}=\frac{\delta\Omega}{\delta\xi}\bigg|_{\rm eq}=\frac{\delta F}{\delta\xi}\bigg|_{\rm eq}+\left(\gamma\int d^3r\left\{\frac{\delta n(\boldsymbol{r})}{\delta\xi}\right\}\right)\bigg|_{\rm eq}. \tag{A8}$$

The kinetic-entropic term can be rewritten as

$$\Delta F_1^0=g_s\sum_j\left(f^F_{n_0,T}(E_j)E_j-TS_{n_0,T}(E_j)\right)+g_s\sum\!\!\!\!\!\!\int\frac{d^3k}{(2\pi)^3}\left\{\left(f^F_{n_0,T}(E_k)E_k-TS_{n_0,T}(E_k)\right)C_{\mathbf{k},s}\right\}+\int d^3r\{v(\boldsymbol{r})n(\boldsymbol{r})\}, \tag{A9}$$

where

$$C_{\mathbf{k},s}\equiv\int d^3r\left\{|\varphi_{\mathbf{k},s}(\boldsymbol{r})|^2-\left|\varphi^0_{\mathbf{k},s}(\boldsymbol{r})\right|^2\right\}. \tag{A10}$$

Thus its derivative is

$$\frac{\delta\Delta F_1^0}{\delta\xi}=\frac{\partial}{\partial\xi}g_s\sum_j\left(f^F_{n_0,T}(E_j)E_j-TS_{n_0,T}(E_j)\right)+\frac{\delta}{\delta\xi}g_s\sum\!\!\!\!\!\!\int\frac{d^3k}{(2\pi)^3}\left\{\left(f^F_{n_0,T}(E_k)E_k-TS_{n_0,T}(E_k)\right)\times C_{\mathbf{k},s}\right\}+\int d^3r\left\{v(\boldsymbol{r})\frac{\delta n(\boldsymbol{r})}{\delta\xi}\right\}. \tag{A11}$$

Using the relation for the entropy expression,

$$\frac{\partial S_{n_0,T}(E)}{\partial\xi}=\frac{E-\mu_{n_0}}{T}\frac{\partial f^F_{n_0,T}(E)}{\partial\xi}, \tag{A12}$$

we find

$$\frac{\delta\Delta F_1^0}{\delta\xi} = g_s \sum_j \left(f^F_{n_0,T}(E_j)\frac{\partial E_j}{\partial\xi} - \frac{\partial T}{\partial\xi} S_{n_0,T}(E_j) \right) + g_s \sum\!\!\!\!\!\!\int \frac{d^3k}{(2\pi)^3} \left\{ \left(f^F_{n_0,T}(E_k)\frac{\partial E_k}{\partial\xi} - \frac{\partial T}{\partial\xi} S_{n_0,T}(E_k) \right) C_{\mathbf{k},s} \right\} + g_s \sum\!\!\!\!\!\!\int \frac{d^3k}{(2\pi)^3} \left\{ \left(f^F_{n_0,T}(E_k)E_k - T S_{n_0,T}(E_k) \right) \frac{\delta C_{\mathbf{k},s}}{\delta\xi} \right\} + \int d^3r \left\{ \left(\mu_{n_0} + v(\boldsymbol{r}) \right) \frac{\delta n(\boldsymbol{r})}{\delta\xi} \right\}. \tag{A13}$$

For the electrostatic and exchange-correlation, we get

$$\frac{\delta\Delta F_1^{\mathrm{el}}}{\delta\xi} = \int d^3r \left\{ v_{\mathrm{el}}(\boldsymbol{r}) \frac{\delta n(\boldsymbol{r})}{\delta\xi} \right\}, \tag{A14}$$

$$\frac{\delta\Delta F_1^{\mathrm{xc}}}{\delta\xi} = \int d^3r \left\{ \left.\frac{\partial f_{\mathrm{xc}}(n)}{\partial\xi}\right|_{n=n(\boldsymbol{r})} - \left.\frac{\partial f_{\mathrm{xc}}(n)}{\partial\xi}\right|_{n=n_0} \right\} + \int d^3r \left\{ v_{\mathrm{xc}}(n(\boldsymbol{r})) \frac{\delta n(\boldsymbol{r})}{\delta\xi} \right\}, \tag{A15}$$

where $f_{\mathrm{xc}}(n)$ is a shorthand notation for $f_{\mathrm{xc}}(n,T,e^2,m)$.

Finally, using the equilibrium relation of Eq. (21), we obtain

$$\frac{\partial F^{\mathrm{eq}}}{\partial\xi} = g_s \sum_j \left(f^F_{n_0,T}(E_j)\frac{\partial E_j}{\partial\xi} - \frac{\partial T}{\partial\xi} S_{n_0,T}(E_j) \right) + g_s \sum\!\!\!\!\!\!\int \frac{d^3k}{(2\pi)^3} \left\{ \left(f^F_{n_0,T}(E_k)\frac{\partial E_k}{\partial\xi} - \frac{\partial T}{\partial\xi} S_{n_0,T}(E_k) \right) C_{\mathbf{k},s} \right\} + g_s \sum\!\!\!\!\!\!\int \frac{d^3k}{(2\pi)^3} \left\{ \left(f^F_{n_0,T}(E_k)E_k - T S_{n_0,T}(E_k) \right) \frac{\delta C_{\mathbf{k},s}}{\delta\xi} \right\}. \tag{A16}$$

The derivative with respect to the temperature T can be rewritten as

$$\frac{\partial F^{\mathrm{eq}}}{\partial T} = \frac{1}{n_i} \left(\frac{\partial f_0^0(n,T,m)}{\partial T} + \frac{\partial f_{\mathrm{xc}}(n,T,e^2,m)}{\partial T} \right)\Bigg|_{n=n_0^{\mathrm{eq}}} + \left(g_s \sum_j \left(-S_{n_0,T}(E_j) \right) + g_s \sum\!\!\!\!\!\!\int \frac{d^3k}{(2\pi)^3} \{ (-S_{n_0,T}(E_k)) C_{\mathbf{k},s} \} \right)\Bigg|_{\mathrm{eq}} + \int d^3r \left\{ \left.\frac{\partial f_{\mathrm{xc}}(n)}{\partial T}\right|_{n=n(\boldsymbol{r})} - \left.\frac{\partial f_{\mathrm{xc}}(n)}{\partial T}\right|_{n=n_0} \right\}\Bigg|_{\mathrm{eq}} \tag{A17}$$

and the derivative with respect to the electron mass m gives

$$\frac{\partial F^{\mathrm{eq}}}{\partial m} = \frac{1}{n_i} \left(\frac{\partial f_0^0(n,T,m)}{\partial m} + \frac{\partial f_{\mathrm{xc}}(n,T,e^2,m)}{\partial m} \right)\Bigg|_{n=n_0^{\mathrm{eq}}} + g_s \sum_j \left(f^F_{n_0,T}(E_j)\frac{\partial E_j}{\partial m} \right) + g_s \sum\!\!\!\!\!\!\int \frac{d^3k}{(2\pi)^3} \left\{ \left(f^F_{n_0,T}(E_k)\frac{\partial E_k}{\partial m} \right) C_{\mathbf{k},s} \right\} + g_s \sum\!\!\!\!\!\!\int \frac{d^3k}{(2\pi)^3} \left\{ \left(f^F_{n_0,T}(E_k)E_k - T S_{n_0,T}(E_k) \right) \frac{\delta C_{\mathbf{k},s}}{\delta m} \right\} + \int d^3r \left\{ \left.\frac{\partial f_{\mathrm{xc}}(n)}{\partial m}\right|_{n=n(\boldsymbol{r})} - \left.\frac{\partial f_{\mathrm{xc}}(n)}{\partial m}\right|_{n=n_0} \right\}\Bigg|_{\mathrm{eq}}. \tag{A18}$$

We have

$$\frac{\partial\tilde{H}}{\partial m} = \frac{\partial\tilde{H}^0}{\partial m} \tag{A19}$$

from which one obtains

$$\frac{\delta}{\delta m} C_{\mathbf{k},s} = 0. \tag{A20}$$

We finally obtain:

$$\frac{\partial F^{\mathrm{eq}}}{\partial m} = \frac{1}{n_i} \left(\frac{\partial f_0^0(n,T,m)}{\partial m} + \frac{\partial f_{\mathrm{xc}}(n,T,e^2,m)}{\partial m} \right)\Bigg|_{n=n_0^{\mathrm{eq}}} + g_s \sum_j \left(f^F_{n_0,T}(E_j)\langle\varphi_j|\frac{\partial\tilde{H}^0}{\partial m}|\varphi_j\rangle \right) + g_s \sum\!\!\!\!\!\!\int \frac{d^3k}{(2\pi)^3} \left\{ f^F_{n_0,T}(E_k) \left(\langle\varphi_{\mathbf{k},s}|\frac{\partial\tilde{H}^0}{\partial m}|\varphi_{\mathbf{k},s}\rangle - \langle\varphi^0_{\mathbf{k},s}|\frac{\partial\tilde{H}^0}{\partial m}|\varphi^0_{\mathbf{k},s}\rangle \right) \right\} + \int d^3r \left\{ \left.\frac{\partial f_{\mathrm{xc}}(n)}{\partial m}\right|_{n=n(\boldsymbol{r})} - \left.\frac{\partial f_{\mathrm{xc}}(n)}{\partial m}\right|_{n=n_0} \right\}\Bigg|_{\mathrm{eq}}. \tag{A21}$$

3. Case of e^2

The derivative with respect to the squared electron charge e^2 is much simpler as the electron density and kinetic-entropic contribution functionals do not depend on it,

$$\frac{\partial F^{\mathrm{eq}}}{\partial(e^2)} = \left.\frac{\delta\Omega}{\delta(e^2)}\right|_{\mathrm{eq}} = \left.\frac{\delta F}{\delta(e^2)}\right|_{\mathrm{eq}}. \tag{A22}$$

We immediately get

$$\frac{\partial F^{\mathrm{eq}}}{\partial(e^2)} = \frac{1}{n_i} \left.\frac{\partial f_{\mathrm{xc}}(n,T,e^2,m)}{\partial(e^2)}\right|_{n=n_0^{\mathrm{eq}}} + \frac{1}{e^2}\left.\Delta F_1^{\mathrm{el}}\right|_{\mathrm{eq}} + \int d^3r \left\{ \left.\frac{\partial f_{\mathrm{xc}}(n)}{\partial(e^2)}\right|_{n=n(\boldsymbol{r})} - \left.\frac{\partial f_{\mathrm{xc}}(n)}{\partial(e^2)}\right|_{n=n_0} \right\}\Bigg|_{\mathrm{eq}}. \tag{A23}$$

APPENDIX B: TRANSFORMATION OF THE ELECTROSTATIC TERM OF THE VIRIAL RELATION

Due to the spherical symmetry of our system, the electron density $n(r)$ and electrostatic potential $v_{\rm el}(r)$ are functions of the radius modulus r,

$$I_{\rm el} \equiv -\int_0^\infty dr \left\{4\pi r^3 n(\boldsymbol{r}) \frac{d}{dr} v_{\rm el}(r)\right\}. \tag{B1}$$

We define the reduced electrostatic potential $\chi_{\rm el}(r)$ such that $v_{\rm el}(r) = Z\chi_{\rm el}(r)/r$,

$$\begin{aligned} I_{\rm el} = &\int_0^\infty dr \left\{4\pi r^2 \big(n(\boldsymbol{r}) - n_0\theta\big(r - R_{\rm WS}^{n_i}\big)\big) \frac{Z\chi_{\rm el}(r)}{r}\right\} \\ &- \int_0^\infty dr \left\{4\pi r^2 \big(n(\boldsymbol{r}) - n_0\theta\big(r - R_{\rm WS}^{n_i}\big)\big) Z \frac{d\chi_{\rm el}(r)}{dr}\right\} \\ &- \int_0^\infty dr \left\{4\pi r^3 n_0 \theta\big(r - R_{\rm WS}^{n_i}\big) \frac{d}{dr} v_{\rm el}(r)\right\}. \end{aligned} \tag{B2}$$

Integrating by parts the third term of the above equation and using the definition of $R_{\rm WS}^{n_i}$, we obtain

$$\begin{aligned} &-\int_0^\infty dr \left\{4\pi r^3 n_0 \theta\big(r - R_{\rm WS}^{n_i}\big) \frac{d}{dr} v_{\rm el}(r)\right\} \\ &\quad = 3\frac{n_0}{n_i} v_{\rm el}\big(R_{\rm WS}^{n_i}\big) + 3n_0 \int_{R_{\rm WS}^{n_i}}^\infty dr\{4\pi r^2 v_{\rm el}(r)\}. \end{aligned} \tag{B3}$$

As concerns the second term of Eq. (B2), it can be shown that if $v_{\rm el}(r)$ and $n(r) - n_0\theta(r - R_{\rm WS}^{n_i})$ fulfill the Poisson equation and boundary conditions,

$$\frac{d^2\chi_{\rm el}(r)}{dr^2} = \frac{4\pi}{Z} r\big(n(r) - n_0\theta\big(r - R_{\rm WS}^{n_i}\big)\big), \tag{B4}$$

$$\chi_{\rm el}(0) = 1, \tag{B5}$$

$$\chi_{\rm el}(r \to \infty) = 0, \tag{B6}$$

$$\left.\frac{d\chi_{\rm el}(r)}{dr}\right|_{r\to\infty} = 0, \tag{B7}$$

then we get

$$\begin{aligned} &\int_0^\infty dr \left\{4\pi r^2 \big(n(r) - n_0\theta\big(r - R_{\rm WS}^{n_i}\big)\big) Z \frac{d\chi_{\rm el}(r)}{dr}\right\} \\ &\quad = \frac{Z^2}{2} \left.\frac{d\chi_{\rm el}(r)}{dr}\right|_{r=0} \\ &\qquad + \frac{1}{2}\int_0^\infty dr \left\{4\pi r^2 \big(n(r) - n_0\theta\big(r - R_{\rm WS}^{n_i}\big)\big) \frac{Z\chi_{\rm el}(r)}{r}\right\}. \end{aligned} \tag{B8}$$

This results from splitting the integral in two terms and integrating one of them by parts. Adding the right-hand side of the preceding equation to the first term of Eq. (B2), we obtain the opposite of the electrostatic part of the energy: $-\Delta F_1^{\rm el}$.

Finally, we get the relation

$$I_{\rm el} = -\Delta F_1^{\rm el} + 3\frac{n_0}{n_i} v_{\rm el}\big(R_{\rm WS}^{n_i}\big) + 3n_0 \int_{R_{\rm WS}^{n_i}}^\infty dr\{4\pi r^2 v_{\rm el}(r)\}. \tag{B9}$$

APPENDIX C: TRANSFORMATION OF THE LDA EXCHANGE-CORRELATION TERM OF THE VIRIAL RELATION

$$I_{\rm xc} \equiv \int d^3r\{n(\boldsymbol{r})\boldsymbol{r}\cdot\nabla(v_{\rm xc}(n(\boldsymbol{r})) - v_{\rm xc}(n_0))\}. \tag{C1}$$

Using the definition of the exchange-correlation potential and integrating by parts, one obtains

$$\begin{aligned} I_{\rm xc} = &-3\int d^3r \left\{\left(n\frac{\partial f_{\rm xc}(n)}{\partial n}\right)\Big|_{n(\boldsymbol{r})} - n(\boldsymbol{r})v_{\rm xc}(n_0)\right\} \\ &- \int d^3r\,\{\boldsymbol{r}\cdot\nabla(f_{\rm xc}(n(\boldsymbol{r})) - n(\boldsymbol{r})v_{\rm xc}(n_0))\} \end{aligned} \tag{C2}$$

$$\begin{aligned} = &\,3v_{\rm xc}(n_0)\int d^3r\{n(\boldsymbol{r}) - n_0\} \\ &+ v_{\rm xc}(n_0)\int d^3r\{\boldsymbol{r}\cdot\nabla(n(\boldsymbol{r}) - n_0)\} \\ &- 3\int d^3r \left\{\left(n\frac{\partial f_{\rm xc}(n)}{\partial n}\right)\Big|_{n(\boldsymbol{r})} - \left(n\frac{\partial f_{\rm xc}(n)}{\partial n}\right)\Big|_{n_0}\right\} \\ &+ \int d^3r\,\{\boldsymbol{r}\cdot\nabla\,(f_{\rm xc}(n(\boldsymbol{r})) - f_{\rm xc}(n_0))\}. \end{aligned} \tag{C3}$$

Finally, integrating the second and fourth terms by parts, and taking into account Eq. (16), one gets

$$\begin{aligned} I_{\rm xc} = &\,3\Delta F_1^{\rm xc} - 3\int d^3r \left\{\left(n\frac{\partial f_{\rm xc}(n)}{\partial n}\right)\Big|_{n(\boldsymbol{r})} \right. \\ &\left. - \left(n\frac{\partial f_{\rm xc}(n)}{\partial n}\right)\Big|_{n_0}\right\}. \end{aligned} \tag{C4}$$

APPENDIX D: VIRIAL RELATIONS FROM THE SCHRÖDINGER AND DIRAC EQUATIONS

1. Schrödinger equation case

We follow here Ref. [66]. Starting from the Schrödinger equation and its complex conjugate, we extract the Clausius virial term $(\boldsymbol{r}\nabla v(\boldsymbol{r}))\varphi^*(\boldsymbol{r})\varphi(\boldsymbol{r})$. We obtain

$$\begin{aligned} &\varphi^*(\boldsymbol{r})\boldsymbol{r}\cdot\nabla\left(-\frac{\hbar^2}{2m}\nabla^2\varphi(\boldsymbol{r})\right) \\ &\quad = \varphi^*(\boldsymbol{r})\,(E + v(\boldsymbol{r}))\,\boldsymbol{r}\cdot\nabla\varphi(\boldsymbol{r}) + (\boldsymbol{r}\cdot\nabla v(\boldsymbol{r}))\,\varphi^*(\boldsymbol{r})\varphi(\boldsymbol{r}), \end{aligned} \tag{D1}$$

$$= \left(-\frac{\hbar^2}{2m}\nabla^2\varphi^*(\boldsymbol{r})\right)\boldsymbol{r}\cdot\nabla\varphi(\boldsymbol{r}) + (\boldsymbol{r}\cdot\nabla v(\boldsymbol{r}))\,\varphi^*(\boldsymbol{r})\varphi(\boldsymbol{r}), \tag{D2}$$

$$\begin{aligned} &-\frac{\hbar^2}{2m}\big(\varphi^*(\boldsymbol{r})\boldsymbol{r}\cdot\nabla\left(\nabla^2\varphi(\boldsymbol{r})\right) + \left(\nabla^2\varphi^*(\boldsymbol{r})\right)\boldsymbol{r}\cdot\nabla\varphi(\boldsymbol{r})\big) \\ &\quad = (\boldsymbol{r}\cdot\nabla v(\boldsymbol{r}))\,\varphi^*(\boldsymbol{r})\varphi(\boldsymbol{r}). \end{aligned} \tag{D3}$$

The following useful relation appears (we use here the Einstein summation convention):

$$\begin{aligned} &\partial_i(\varphi^*(\boldsymbol{r})\partial_i(x_j\partial_j\varphi(\boldsymbol{r})) - (\partial_i\varphi^*(\boldsymbol{r}))(x_j\partial_j\varphi(\boldsymbol{r}))) \\ &\quad = (\partial_i\varphi^*(\boldsymbol{r}))\partial_i(x_j\partial_j\varphi(\boldsymbol{r})) + \varphi^*(\boldsymbol{r})\partial_i\partial_i(x_j\partial_j\varphi(\boldsymbol{r})) \\ &\qquad - (\partial_i\partial_i\varphi^*(\boldsymbol{r}))(x_j\partial_j\varphi(\boldsymbol{r})) - (\partial_i\varphi^*(\boldsymbol{r}))\partial_i(x_j\partial_j\varphi(\boldsymbol{r})), \end{aligned} \tag{D4}$$

$$= \varphi^*(\boldsymbol{r})\partial_i\partial_i(x_j\partial_j\varphi(\boldsymbol{r})) - (\partial_i\partial_i\varphi^*(\boldsymbol{r}))(x_j\partial_j\varphi(\boldsymbol{r})), \quad \text{(D5)}$$

$$= \varphi^*(\boldsymbol{r})(\partial_i\partial_i\varphi(\boldsymbol{r}) + \partial_i(x_j\partial_i\partial_j\varphi(\boldsymbol{r}))) - (\partial_i\partial_i\varphi^*(\boldsymbol{r}))(x_j\partial_j\varphi(\boldsymbol{r})), \quad \text{(D6)}$$

$$= 2\varphi^*(\boldsymbol{r})\partial_i\partial_i\varphi(\boldsymbol{r}) + \varphi^*(\boldsymbol{r})x_j\partial_j\partial_i\partial_i\varphi(\boldsymbol{r}) - (\partial_i\partial_i\varphi^*(\boldsymbol{r}))(x_j\partial_j\varphi(\boldsymbol{r})). \quad \text{(D7)}$$

Using Eq. (D7) in Eq. (D3), we obtain

$$-\frac{\hbar^2}{2m}(\nabla\cdot(\varphi^*(\boldsymbol{r})\nabla(\boldsymbol{r}\cdot\nabla\varphi(\boldsymbol{r})) - (\nabla\varphi^*(\boldsymbol{r}))(\boldsymbol{r}\cdot\nabla\varphi(\boldsymbol{r}))) - 2\varphi^*(\boldsymbol{r})\nabla^2\varphi(\boldsymbol{r})) = (\boldsymbol{r}\cdot\nabla v(\boldsymbol{r}))\varphi^*(\boldsymbol{r})\varphi(\boldsymbol{r}). \quad \text{(D8)}$$

In the case of plane waves, we get

$$-\frac{\hbar^2}{2m}\left(\nabla\cdot\left(\varphi^{0*}(\boldsymbol{r})\nabla\left(\boldsymbol{r}\cdot\nabla\varphi^0(\boldsymbol{r})\right) - \left(\nabla\varphi^{0*}(\boldsymbol{r})\right)\left(\boldsymbol{r}\cdot\nabla\varphi^0(\boldsymbol{r})\right)\right) - 2\varphi^{0*}(\boldsymbol{r})\nabla^2\varphi^0(\boldsymbol{r})\right) = 0. \quad \text{(D9)}$$

2. Dirac equation case

In the case of the Dirac equation, we follow Ref. [67]. Starting from the Dirac equation and its Hermitian conjugate, we extract the Clausius virial term $(\boldsymbol{r}\cdot\nabla v(\boldsymbol{r}))\varphi^\dagger(\boldsymbol{r})\varphi(\boldsymbol{r})$. We get

$$\varphi^\dagger(\boldsymbol{r})\boldsymbol{r}\cdot\nabla(-i\hbar c\boldsymbol{\alpha}\cdot\nabla\varphi(\boldsymbol{r}) + mc^2\beta\varphi(\boldsymbol{r})) = \varphi^\dagger(\boldsymbol{r})(E + v(\boldsymbol{r}))\boldsymbol{r}\cdot\nabla\varphi(\boldsymbol{r}) + (\boldsymbol{r}\cdot\nabla v(\boldsymbol{r}))\varphi^\dagger(\boldsymbol{r})\varphi(\boldsymbol{r}) \quad \text{(D10)}$$

$$= (i\hbar c(\nabla\varphi^\dagger(\boldsymbol{r}))\cdot\boldsymbol{\alpha} + mc^2\varphi^\dagger(\boldsymbol{r})\beta)\boldsymbol{r}\cdot\nabla\varphi(\boldsymbol{r}) + (\boldsymbol{r}\cdot\nabla v(\boldsymbol{r}))\varphi^\dagger(\boldsymbol{r})\varphi(\boldsymbol{r}). \quad \text{(D11)}$$

The above can be simplified and rewritten as

$$-i\hbar c(\varphi^\dagger(\boldsymbol{r})\boldsymbol{r}\cdot\nabla(\boldsymbol{\alpha}\cdot\nabla\varphi(\boldsymbol{r})) + \left(\nabla\varphi^\dagger(\boldsymbol{r})\right)\cdot\boldsymbol{\alpha}\,\boldsymbol{r}\cdot\nabla\varphi(\boldsymbol{r})) = (\boldsymbol{r}\cdot\nabla v(\boldsymbol{r}))\varphi^\dagger(\boldsymbol{r})\varphi(\boldsymbol{r}). \quad \text{(D12)}$$

The following transformation is then useful (we use again the Einstein summation convention):

$$\partial_j(\varphi^\dagger(\boldsymbol{r})\alpha_j(x_i\partial_i\varphi(\boldsymbol{r}))) = (\partial_j\varphi^\dagger(\boldsymbol{r}))\alpha_j(x_i\partial_i\varphi(\boldsymbol{r})) + \varphi^\dagger(\boldsymbol{r})\alpha_j\partial_j(x_i\partial_i\varphi(\boldsymbol{r})) \quad \text{(D13)}$$

$$= (\partial_j\varphi^\dagger(\boldsymbol{r}))\alpha_j(x_i\partial_i\varphi(\boldsymbol{r})) + \varphi^\dagger(\boldsymbol{r})\alpha_j(\partial_j x_i)(\partial_i\varphi(\boldsymbol{r})) + \varphi^\dagger(\boldsymbol{r})\alpha_j x_i(\partial_j\partial_i\varphi(\boldsymbol{r})) \quad \text{(D14)}$$

$$= x_i(\varphi^\dagger(\boldsymbol{r})\alpha_j\partial_i\partial_j\varphi(\boldsymbol{r}) + (\partial_j\varphi^\dagger(\boldsymbol{r}))\alpha_j(\partial_i\varphi(\boldsymbol{r}))) + \varphi^\dagger(\boldsymbol{r})\alpha_j\delta_{ij}\partial_i\varphi(\boldsymbol{r}). \quad \text{(D15)}$$

Thus we obtain

$$x_i(\varphi^\dagger(\boldsymbol{r})\alpha_j\partial_i\partial_j\varphi(\boldsymbol{r}) + (\partial_j\varphi^\dagger(\boldsymbol{r}))\alpha_j(\partial_i\varphi(\boldsymbol{r}))) = \partial_j(\varphi^\dagger(\boldsymbol{r})\alpha_j(x_i\partial_i\varphi(\boldsymbol{r}))) - \varphi^\dagger(\boldsymbol{r})\alpha_j\partial_j\varphi(\boldsymbol{r}). \quad \text{(D16)}$$

Using Eq. (D16) in Eq. (D12), we have

$$-i\hbar c(\nabla\cdot(\varphi^\dagger(\boldsymbol{r})\boldsymbol{\alpha}(\boldsymbol{r}\cdot\nabla\varphi(\boldsymbol{r}))) - \varphi^\dagger(\boldsymbol{r})\boldsymbol{\alpha}\cdot\nabla\varphi(\boldsymbol{r})) = (\boldsymbol{r}\cdot\nabla v(\boldsymbol{r}))\varphi^\dagger(\boldsymbol{r})\varphi(\boldsymbol{r}). \quad \text{(D17)}$$

In the case of plane waves, we get

$$-i\hbar c(\nabla\cdot(\varphi^{0\dagger}(\boldsymbol{r})\boldsymbol{\alpha}(\boldsymbol{r}\cdot\nabla\varphi^0(\boldsymbol{r}))) - \varphi^{0\dagger}(\boldsymbol{r})\boldsymbol{\alpha}\cdot\nabla\varphi^0(\boldsymbol{r})) = 0. \quad \text{(D18)}$$

APPENDIX E: TREATMENT OF THE SURFACE TERM IN THE FRAMEWORK OF ATOM-IN-JELLIUM CALCULATIONS

1. Schrödinger equation case

$$I_S = -\frac{\hbar^2}{2m}\int_{\Sigma_\infty} \boldsymbol{dS}\cdot\{\varphi^*_{E,\ell,m}(\boldsymbol{r})\nabla(\boldsymbol{r}\cdot\nabla\varphi_{E,\ell,m}(\boldsymbol{r})) - (\nabla\varphi^*_{E,\ell,m}(\boldsymbol{r}))(\boldsymbol{r}\cdot\nabla\varphi_{E,\ell,m}(\boldsymbol{r})) - \varphi^{0*}_{E,\ell,m}(\boldsymbol{r})\nabla\left(\boldsymbol{r}\cdot\nabla\varphi^0_{E,\ell,m}(\boldsymbol{r})\right) + \left(\nabla\varphi^{0*}_{E,\ell,m}(\boldsymbol{r})\right)\left(\boldsymbol{r}\cdot\nabla\varphi^0_{E,\ell,m}(\boldsymbol{r})\right)\}. \quad \text{(E1)}$$

We integrate over Σ_∞, which is a sphere of radius $r\to\infty$. The elementary surface is $\boldsymbol{dS} = r\sin\theta d\theta d\phi\,\boldsymbol{r}$. We have

$$I_S = -\frac{\hbar^2}{2m}\lim_{r\to\infty}\int_0^\pi\int_0^{2\pi} d\theta d\phi r\sin\theta \times\{\varphi^*_{E,\ell,m}(\boldsymbol{r})\boldsymbol{r}\cdot\nabla(\boldsymbol{r}\cdot\nabla\varphi_{E,\ell,m}(\boldsymbol{r})) - (\boldsymbol{r}\cdot\nabla\varphi^*_{E,\ell,m}(\boldsymbol{r}))(\boldsymbol{r}\cdot\nabla\varphi_{E,\ell,m}(\boldsymbol{r})) - \varphi^{0*}_{E,\ell,m}(\boldsymbol{r})\boldsymbol{r}\cdot\nabla\left(\boldsymbol{r}\cdot\nabla\varphi^0_{E,\ell,m}(\boldsymbol{r})\right) + \left(\boldsymbol{r}\cdot\nabla\varphi^{0*}_{E,\ell,m}(\boldsymbol{r})\right)\left(\boldsymbol{r}\cdot\nabla\varphi^0_{E,\ell,m}(\boldsymbol{r})\right)\}. \quad \text{(E2)}$$

The continuum and plane-wave wave functions can be expressed, respectively, as $\varphi_{E,\ell,m}(\boldsymbol{r}) = R_{E,\ell}(r)Y_{\ell,m}(\theta,\phi)/r$ and $\varphi^0_{E,\ell,m}(\boldsymbol{r}) = R^0_{E,\ell}(r)Y_{\ell,m}(\theta,\phi)/r$ with the $Y_{\ell,m}(\theta,\phi)$ being the spherical harmonics,

$$I_S = -\frac{\hbar^2}{2m}\int_0^\pi\int_0^{2\pi} d\theta d\phi\sin\theta\{|Y_{\ell,m}(\theta,\phi)|^2\} \times\lim_{r\to\infty} r\left\{\frac{R_{E,\ell}(r)}{r}r\frac{\partial}{\partial r}\left(r\frac{\partial}{\partial r}\left(\frac{R_{E,\ell}(r)}{r}\right)\right) - \left(r\frac{\partial}{\partial r}\left(\frac{R_{E,\ell}(r)}{r}\right)\right)^2 - \frac{R^0_{E,\ell}(r)}{r}r\frac{\partial}{\partial r}\left(r\frac{\partial}{\partial r}\left(\frac{R^0_{E,\ell}(r)}{r}\right)\right) + \left(r\frac{\partial}{\partial r}\left(\frac{R^0_{E,\ell}(r)}{r}\right)\right)^2\right\}. \quad \text{(E3)}$$

We have $R_{E,\ell}(r\to\infty) = A_E\sin(p_E r - \ell\pi/2 + \Delta_{E,\ell})$ and $R^0_{E,\ell}(r\to\infty) = A_E\sin(p_E r - \ell\pi/2)$,

$$I_S = -\frac{\hbar^2}{2m}\int_0^\pi\int_0^{2\pi} d\theta d\phi\sin\theta\{|Y_{\ell,m}(\theta,\phi)|^2\} \times\lim_{r\to\infty} A_E^2 p_E(\sin(2p_E r - \ell\pi + 2\Delta_{E,\ell}) - \sin(2p_E r - \ell\pi)) \quad \text{(E4)}$$

$$= -\frac{\hbar^2}{2m}\int_0^\pi\int_0^{2\pi} d\theta d\phi\sin\theta\{|Y_{\ell,m}(\theta,\phi)|^2\} \times\lim_{r\to\infty} 2A_E^2 p_E\sin\Delta_{E,\ell}\cos(2p_E r - \ell\pi + \Delta_{E,\ell}). \quad \text{(E5)}$$

In the preceding equation for I_S we find the same rapidly oscillating term as that encountered in the Friedel sum rule. Integrated over the energy E, it leads to a zero contribution.

2. Dirac equation case

$$I_S = -i\hbar c \int_{\Sigma_\infty} \boldsymbol{dS} \cdot \left\{ \varphi^\dagger_{E,\kappa,m}(\boldsymbol{r}) \boldsymbol{\alpha} (\boldsymbol{r} \cdot \boldsymbol{\nabla} \varphi_{E,\kappa,m}(\boldsymbol{r})) - \varphi^{0\dagger}_{E,\kappa,m}(\boldsymbol{r}) \boldsymbol{\alpha} \left(\boldsymbol{r} \cdot \boldsymbol{\nabla} \varphi^0_{E,\kappa,m}(\boldsymbol{r}) \right) \right\}. \tag{E6}$$

Here again we consider a sphere of radius $r \to \infty$. The elementary surface is $\boldsymbol{dS} = r^2 \sin\theta d\theta d\phi \boldsymbol{e_r}$, where $\boldsymbol{e_r} \equiv \boldsymbol{r}/r$. We have

$$I_S = -i\hbar c \lim_{r\to\infty} \int_0^\pi \int_0^{2\pi} d\theta d\phi r^2 \sin\theta \times \left\{ \varphi^\dagger_{E,\kappa,m}(\boldsymbol{r}) \boldsymbol{e_r} \cdot \boldsymbol{\alpha} (\boldsymbol{r} \cdot \boldsymbol{\nabla} \varphi_{E,\kappa,m}(\boldsymbol{r})) - \varphi^{0\dagger}_{E,\kappa,m}(\boldsymbol{r}) \boldsymbol{e_r} \cdot \boldsymbol{\alpha} (\boldsymbol{r} \cdot \boldsymbol{\nabla} \varphi^0_{E,\kappa,m}(\boldsymbol{r})) \right\}. \tag{E7}$$

The continuum and plane-wave bispinors can be expressed, respectively, as

$$\varphi_{E,\kappa,m}(\boldsymbol{r}) = \begin{pmatrix} i \dfrac{P_{E,\kappa}(r)}{r} \Omega_{\kappa,m}(\theta,\phi) \\ \dfrac{Q_{E,\kappa}(r)}{r} \Omega_{-\kappa,m}(\theta,\phi) \end{pmatrix}$$

and

$$\varphi^0_{E,\kappa,m}(\boldsymbol{r}) = \begin{pmatrix} i \dfrac{P^0_{E,\kappa}(r)}{r} \Omega_{\kappa,m}(\theta,\phi) \\ \dfrac{Q^0_{E,\kappa}(r)}{r} \Omega_{-\kappa,m}(\theta,\phi) \end{pmatrix}$$

with the $\Omega_{\kappa,m}(\theta,\phi)$ being the spherical spinors.

$$I_S = -i\hbar c \lim_{r\to\infty} \int_0^\pi \int_0^{2\pi} d\theta d\phi r^2 \sin\theta \left\{ \begin{pmatrix} -i \frac{P_{E,\kappa}(r)}{r} \Omega^\dagger_{\kappa,m} & \frac{Q_{E,\kappa}(r)}{r} \Omega^\dagger_{-\kappa,m} \end{pmatrix} \begin{pmatrix} 0 & \boldsymbol{e_r}\cdot\boldsymbol{\sigma} \\ \boldsymbol{e_r}\cdot\boldsymbol{\sigma} & 0 \end{pmatrix} \begin{pmatrix} i\Omega_{\kappa,m} r \frac{\partial}{\partial r} \left(\frac{P_{E,\kappa}(r)}{r} \right) \\ \Omega_{-\kappa,m} r \frac{\partial}{\partial r} \left(\frac{Q_{E,\kappa}(r)}{r} \right) \end{pmatrix} - \begin{pmatrix} -i \frac{P^0_{E,\kappa}(r)}{r} \Omega^\dagger_{\kappa,m} & \frac{Q^0_{E,\kappa}(r)}{r} \Omega^\dagger_{-\kappa,m} \end{pmatrix} \begin{pmatrix} 0 & \boldsymbol{e_r}\cdot\boldsymbol{\sigma} \\ \boldsymbol{e_r}\cdot\boldsymbol{\sigma} & 0 \end{pmatrix} \begin{pmatrix} i\Omega_{\kappa,m} r \frac{\partial}{\partial r} \left(\frac{P^0_{E,\kappa}(r)}{r} \right) \\ \Omega_{-\kappa,m} r \frac{\partial}{\partial r} \left(\frac{Q^0_{E,\kappa}(r)}{r} \right) \end{pmatrix} \right\} \tag{E8}$$

$$I_S = \hbar c \int_0^\pi \int_0^{2\pi} d\theta d\phi \sin\theta \{ |\Omega_{\kappa,m}(\theta,\phi)|^2 \} \lim_{r\to\infty} r^2 \left(P_{E,\kappa}(r) \frac{\partial}{\partial r} \left(\frac{Q_{E,\kappa}(r)}{r} \right) - P^0_{E,\kappa}(r) \frac{\partial}{\partial r} \left(\frac{Q^0_{E,\kappa}(r)}{r} \right) \right) - \hbar c \int_0^\pi \int_0^{2\pi} d\theta d\phi \sin\theta \{ |\Omega_{-\kappa,m}(\theta,\phi)|^2 \} \lim_{r\to\infty} r^2 \left(Q_{E,\kappa}(r) \frac{\partial}{\partial r} \left(\frac{P_{E,\kappa}(r)}{r} \right) - Q^0_{E,\kappa}(r) \frac{\partial}{\partial r} \left(\frac{P^0_{E,\kappa}(r)}{r} \right) \right), \tag{E9}$$

where we have used the well-known relation $(\boldsymbol{e_r} \cdot \boldsymbol{\sigma}) \Omega_{\kappa,m}(\theta,\phi) = -\Omega_{-\kappa,m}(\theta,\phi)$.

We have $P_{E,\kappa}(r \to \infty) = A_E \sin(p_E r - \ell_\kappa \pi/2 + \Delta_{E,\kappa})$ and $Q_{E,\kappa}(r \to \infty) = -\mathrm{sgn}(\kappa) A_E \frac{p_E}{E+2mc^2} \sin(p_E r - \ell_{-\kappa}\pi/2 + \Delta_{E,\kappa})$, so we get

$$\begin{aligned} I_S &= \hbar c \int_0^\pi \int_0^{2\pi} d\theta d\phi \sin\theta \{ |\Omega_{\kappa,m}(\theta,\phi)|^2 \} \\ &\quad \times \lim_{r\to\infty} \kappa A_E^2 \frac{p_E}{E+2mc^2} (\sin(2p_E - \ell_\kappa \pi + 2\Delta_{E,\kappa}) \\ &\quad - \sin(2p_E - \ell_\kappa \pi)) \end{aligned} \tag{E10}$$

$$\begin{aligned} &= \hbar c \int_0^\pi \int_0^{2\pi} d\theta d\phi \sin\theta \{ |\Omega_{\kappa,m}(\theta,\phi)|^2 \} \\ &\quad \times \lim_{r\to\infty} 2\kappa A_E^2 \frac{p_E}{E+2mc^2} \sin\Delta_{E,\kappa} \\ &\quad \times \cos(2p_E - \ell_\kappa \pi + \Delta_{E,\kappa}). \end{aligned} \tag{E11}$$

APPENDIX F: VARIATION ON e^2 AND m OF THE LDA EXCHANGE-CORRELATION TERM

We define the dimensionless function $\dot{f}$ as

$$f_{\mathrm{xc}}(n,T,e^2,m) \equiv \frac{E_H(e^2,m)}{a_0(e^2,m)^3} \dot{f} \left(n a_0(e^2,m)^3, \frac{k_B T}{E_H(e^2,m)}, e^2, m \right), \tag{F1}$$

where $E_H(e^2,m)$ is the Hartree energy and $a_0(e^2,m)$ is the Bohr radius viewed as functions of the squared electron charge e^2 and of the electron mass m,

$$E_H(e^2,m) \equiv \left(\frac{e^2}{\hbar c} \right)^2 mc^2; \quad a_0(e^2,m) \equiv \frac{\hbar c}{\left(\frac{e^2}{\hbar c}\right) mc^2}. \tag{F2}$$

We assume that the exchange-correlation term depends on e^2 and on m only through the atomic units system, and we suppress any explicit dependence of the function $\dot{f}$ on e^2 and m,

$$\frac{\partial \dot{f}}{\partial (e^2)} = \frac{\partial \dot{f}}{\partial m} = 0. \tag{F3}$$

In this case, we immediately find that

$$e^2\frac{\partial f_{\rm xc}}{\partial(e^2)} = 5f_{\rm xc} - 3n\frac{\partial f_{\rm xc}}{\partial n} - 2T\frac{\partial f_{\rm xc}}{\partial T}, \tag{F4}$$

$$m\frac{\partial f_{\rm xc}}{\partial m} = 4f_{\rm xc} - 3n\frac{\partial f_{\rm xc}}{\partial n} - T\frac{\partial f_{\rm xc}}{\partial T}. \tag{F5}$$

We then obtain the following two useful relations to obtain, respectively, the nonrelativistic and relativistic virial theorems:

$$2u_{\rm xc}(n,T,e^2,m) - u_{\rm xc}^{\rm int}(n,T,e^2,m) = -3f_{\rm xc}(n,T,e^2,m) + 3n\frac{\partial f_{\rm xc}(n,T,e^2,m)}{\partial n}, \tag{F6}$$

$$t_{\rm xc}(n,T,e^2,m) + u_{\rm xc}^{\rm int}(n,T,e^2,m) = -3f_{\rm xc}(n,T,e^2,m) + 3n\frac{\partial f_{\rm xc}(n,T,e^2,m)}{\partial n}. \tag{F7}$$

It is worth stressing that the terms containing the derivative with respect to temperature cancel on the right-hand side in the two preceding relations.

APPENDIX G: EFFECT OF A RELATIVISTIC TREATMENT IN THE CASE OF YTTERBIUM AT 30-EV TEMPERATURE

Figure 14 is provided in order to show the effect of a relativistic treatment on a heavy element (ytterbium) in the warm-dense-matter regime. As can be seen on this figure, this effect appears to be negligible both on the electron pressure and on the mean ionization.

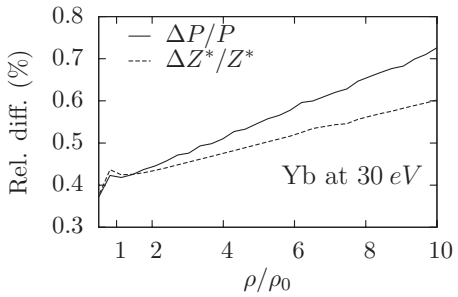

FIG. 14. Effect of a relativistic treatment along the ytterbium 30-eV isotherm. Relatives differences between electron pressures and mean ionizations stemming from a nonrelativistic calculation and from a relativistic calculation are plotted vs the compression ratio (we use $\rho_0 = 7.019\ \mathrm{g\,cm^{-3}}$).

[1] S. Rosseland, *Handbuch der Astrophysik*, Vol. 3, edited by E. A. Milne, A. Pannekoek, S. Rosseland, and W. H. Westphal (J. Springer, Berlin, 1930), chap. 4: The Principles of Quantum Theory.

[2] P. M. Morse, Astrophys. J. **92**, 27 (1940).

[3] T. R. Carson, D. F. Mayers, and D. W. N. Stibbs, Mon. Not. R. Astron. Soc. **140**, 483 (1968).

[4] S. J. Rose, J. Quant. Spectrosc. Radiat. Transfer **71**, 635 (2001).

[5] G. Baym, C. Pethick, and P. Sutherland, Astrophys. J. **170**, 299 (1971).

[6] F. X. Timmes and D. Arnett, Astrophys. J. Suppl. Ser. **125**, 277 (1999).

[7] J. D. Lindl, P. Amendt, R. L. Berger, S. G. Glendinning, S. H. Glenzer, S. W. Haan, R. L. Kauffman, O. L. Landen, and L. J. Suter, Phys. Plasmas **11**, 339 (2004).

[8] J. Giorla, J. Bastian, C. Bayer, B. Canaud, M. Casanova, F. Chaland, C. Cherfils, C. Clique, E. Dattolo, P. Fremerye, D. Galmiche, F. Garaude, P. Gauthier, S. Laffite, N. Lecler, S. Liberatore, P. Loiseau, G. Malinie, L. Masse, A. Masson, M. C. Monteil, F. Poggi, R. Quach, F. Renaud, Y. Saillard, P. Seytor, M. Vandenboomgaerde, J. Van der Vliet, and F. Wagon, Plasma Phys. Controlled Fusion **48**, B75 (2006).

[9] G. O'Sullivan, A. Cummings, P. Dunne, K. Fahy, P. Hayden, L. McKinney, N. Murphy, E. Sokell, and J. White, AIP Conf. Proc. **771**, 108 (2005).

[10] T. Auguste, F. de Gaufridy de Dortan, T. Ceccotti, J. F. Hergott, O. Sublemontier, D. Descamps, and M. Schmidt, J. Appl. Phys. **101**, 043302 (2007).

[11] J. E. Bailey, G. A. Rochau, C. A. Iglesias, J. Abdallah, J. J. MacFarlane, I. Golovkin, P. Wang, R. C. Mancini, P. W. Lake, T. C. Moore, M. Bump, O. Garcia, and S. Mazevet, Phys. Rev. Lett. **99**, 265002 (2007).

[12] G. Loisel, P. Arnault, S. Bastiani-Ceccotti, T. Blenski, T. Caillaud, J. Fariaut, W. Fölsner, F. Gilleron, J.-C. Pain, M. Poirier, C. Reverdin, V. Silvert, F. Thais, S. Turck-Chièze, and B. Villette, High Energy Density Phys. **5**, 173 (2009).

[13] A. Bar-Shalom, J. Oreg, W. H. Goldstein, D. Shvarts, and A. Zigler, Phys. Rev. A **40**, 3183 (1989).

[14] R. P. Feynman, N. Metropolis, and E. Teller, Phys. Rev. **75**, 1561 (1949).

[15] J. C. Slater and H. M. Krutter, Phys. Rev. **47**, 559 (1935).

[16] R. Latter, Phys. Rev. **99**, 510 (1955).

[17] J. W. Zink, Phys. Rev. **176**, 279 (1968).

[18] G. V. Shpatakovskaya, High Temp. **23**, 40 (1985); Teplofiz. Vys. Temp. **23**, 42 (1985).

[19] B. Ritchie, Phys. Plasmas **11**, 3417 (2004).

[20] B. F. Rozsnyai, Phys. Rev. A **5**, 1137 (1972).

[21] D. A. Liberman, Phys. Rev. B **20**, 4981 (1979).

[22] T. Blenski and B. Cichocki, Phys. Rev. E **75**, 056402 (2007).

[23] T. Blenski and B. Cichocki, High Energy Density Phys. **3**, 34 (2007).

[24] R. Piron, T. Blenski, and B. Cichocki, J. Phys. A **42**, 214059 (2009).

[25] R. Piron, T. Blenski, and B. Cichocki, High Energy Density Phys. **5**, 258 (2009).

[26] B. Wilson, V. Sonnad, P. Sterne, and W. Isaacs, J. Quant. Spectrosc. Radiat. Transf. **81**, 499 (2003).

[27] B. Wilson, V. Sonnad, P. Sterne, and W. Isaacs, J. Quant. Spectrosc. Radiat. Transf. **99**, 658 (2006).

[28] F. Perrot (private communication).

[29] S. H. Lee and T. K. Wan, Phys. Rev. B **78**, 224103 (2008).

[30] A. Bar-Shalom, J. Oreg, and M. Klapisch, J. Quant. Spectrosc. Radiat. Transf. **99**, 35 (2006).

[31] A. Barshalom and J. Oreg, High Energy Density Phys. **3**, 12 (2007).
[32] A. Barshalom and J. Oreg, High Energy Density Phys. **5**, 196 (2009).
[33] P. Hohenberg and W. Kohn, Phys. Rev. **136**, B864 (1964).
[34] W. Kohn *et al.*, Phys. Rev. **140**, A1133 (1965).
[35] N. D. Mermin, Phys. Rev. **137**, A1441 (1965).
[36] A. K. Rajagopal, J. Phys. C **11**, L943 (1978).
[37] A. H. MacDonald and S. H. Vosko, J. Phys. C **12**, 2977 (1979).
[38] B. Held and P. Pignolet, J. Phys. (Paris) **47**, 437 (1986).
[39] H. Iyetomi and S. Ichimaru, Phys. Rev. A **34**, 433 (1986).
[40] R. Piron, Ph.D. thesis, École Polytechnique, 2009 (in French, available at [http://tel.archives-ouvertes.fr/tel-00446558/fr/]).
[41] A. F. Nikiforov, V. G. Novikov, and V. B. Uvarov, *Quantum-Statistical Models of Hot Dense Matter* (Birkhauser, Basel, Switzerland, 2005).
[42] T. Blenski and K. Ishikawa, Phys. Rev. E **51**, 4869 (1995).
[43] L. Hedin and B. I. Lundqvist, J. Phys. C **4**, 2064 (1971).
[44] F. Perrot, Phys. Rev. A **20**, 586 (1979).
[45] S. Ichimaru, H. Iyetomi, and S. Tanaka, Phys. Rep. **149**, 91 (1987).
[46] J. Arponen, P. Hautojärvi, R. Nieminen, and E. Pajanne, J. Phys. F **3**, 2092 (1973).
[47] M. Manninen, R. Nieminen, P. Hautojärvi, and J. Arponen, Phys. Rev. B **12**, 4012 (1975).
[48] R. M. Nieminen, J. Phys. F **7**, 375 (1977).
[49] P. A. Sterne, S. B. Hansen, B. Wilson, and W. A. Isaacs, High Energy Density Phys. **3**, 278 (2007).
[50] C. Gouedard and C. Deutsch, J. Math. Phys. **19**, 32 (1978).
[51] E. L. Pollock and J. P. Hansen, Phys. Rev. A **8**, 3110 (1973).
[52] R. G. Greene, H. Luo, and A. L. Ruoff, Phys. Rev. Lett. **73**, 2075 (1994).
[53] P. Renaudin, C. Blancard, J. Clérouin, G. Faussurier, P. Noiret, and V. Recoules, Phys. Rev. Lett. **91**, 075002 (2003).
[54] P. Renaudin, V. Recoules, P. Noiret, and J. Clérouin, Phys. Rev. E **73**, 056403 (2006).
[55] V. N. Korobenko, A. D. Rakhel, A. I. Savvatimski, and V. E. Fortov, Phys. Rev. B **71**, 014208 (2005).
[56] V. N. Korobenko and A. D. Rakhel, Phys. Rev. B **75**, 064208 (2007).
[57] A. V. Bushman, I. V. Lomonosov, K. V. Khishchenko, V. P. Kopyshev, E. A. Kuzmenkov, V. E. Kogan, P. R. Levashov, and I. N. Lomov, Ihed shock wave database [http://www.ihed.ras.ru/rusbank/].
[58] S. P. Lyon, J. D. Johnson, and Group T-1, Sesame, The Los Alamos National Laboratory Equation-of-State Database, Technical Report LA-UR-92-3407, Los Alamos National Laboratory, 1995.
[59] T. L. Loucks, *Augmented Plane Wave Method* (Benjamin, New York, 1967).
[60] H. Szichman and A. D. Krumbein, Phys. Rev. A **33**, 706 (1986).
[61] J. P. Hansen, Phys. Rev. A **8**, 3096 (1973).
[62] A. F. Nikiforov, V. G. Novikov, and V. B. Uvarov, High Temp. **25**, 10 (1987); Teplofiz. Vys. Temp. **25**, 12 (1987).
[63] J.-C. Pain, Contrib. Plasma Phys. **47**, 421 (2007).
[64] R. Clausius, Ann. Phys. (Berlin) **141**, 124 (1870).
[65] V. Fock, Z. Phys. **63**, 855 (1930).
[66] J. C. Slater, J. Chem. Phys. **1**, 687 (1933).
[67] N. H. March, Phys. Rev. **92**, 481 (1953).